Climate Dynamics (2025) 63:89
https://doi.org/10.1007/s00382-024-07563-x

ORIGINAL ARTICLE

# Km-scale climate simulations over Madeira and Canary Islands under present and future conditions: a model intercomparison study

**Marianna Adinolfi[1] · Leo Luca Loprieno[1,2] · Marie-Estelle Demory[2,3,4,5] · Christian Zeman[2] · Christoph Schär[2]**

Received: 28 February 2024 / Accepted: 22 December 2024 / Published online: 16 January 2025


**Abstract**

This study seeks to explore two new km-scale regional climate simulations prepared through the European Climate Prediction project over the Madeira and Canary islands, which are Portuguese and Spanish archipelagos located in the North Atlantic, off the African coast. The simulations are based on two models using different modelling approaches: COSMO-CLM with a three-step nesting at 50, 25 and 3 km grid spacing using a time-slice approach driven by a global climate model, and COSMO-crCLIM with a two-step nesting at 12 and 1 km grid spacing using the pseudo-global warming approach, where the current-day simulations are driven by ERA-Interim reanalysis. Although the modelling approaches are different, several findings are highlighted: (1) the use of km-scale simulation is essential to properly represent temperature and precipitation mean and extremes over small islands that are characterized by complex topography; (2) the projected changes in temperature and precipitation mean and extremes are qualitatively similar in all seasons except autumn; (3) the differences in the autumn projections are shown to be due to the large-scale driving conditions. Small islands, such as the Canary and Madeira ones, are often neglected by large modelling initiatives, so the presented simulations contribute to filling this gap for local policy makers, stakeholders and climate services. The encouraging results highlight the need for further coordinated km-scale projections.

**Keywords** Convection-permitting models · Climate projections over small islands · Elevation-dependent behaviour · Temperature and precipitation extremes

✉ Marianna Adinolfi
marianna.adinolfi@cmcc.it

Leo Luca Loprieno
leo.loprieno@cmcc.it

Marie-Estelle Demory
marie-estelle.demory@wyssacademy.org

Christian Zeman
christian.zeman@env.ethz.ch

Christoph Schär
schaer@env.ethz.ch

1 CMCC Foundation - Euro-Mediterranean Center on Climate Change, Lecce 73100, Italy

2 Institute for Atmospheric and Climate Science, ETH Zürich, Zürich 8092, Switzerland

3 Wyss Academy for Nature, University of Bern, Bern 3011, Switzerland

4 Climate and Environmental Physics, University of Bern, Bern 3012, Switzerland

5 Oeschger Centre for Climate Change Research, University of Bern, Bern 3012, Switzerland

## 1 Introduction

As Earth warms, the intensity of extreme events is increasing worldwide (Pichelli et al. 2021; Weather and climate extreme events in a changing climate 2021). In July 2021, for example, various central European countries experienced some of the most devastating precipitation events in the past few decades, causing an estimated infrastructural damage of several bn (Gallin 2021; Mohr et al. 2023). On the other hand, the months June–July 2023 have caused that summer to be one of the hottest ones due to persisting and recurring anticyclonic situations with record maximum temperatures in the Mediterranean region as well as in the Macaronesian islands (Copernicus 2023). Over the latter, the increasing fire risk associated to the warming climate and large amounts of rainfall pose serious threats. These islands are characterized by a complex topography with large differences in elevation, from sea level to almost 2000 m above sea level (a.s.l.) in Madeira (Fragoso et al. 2012) and almost 4000 m a.s.l. in the Canary islands (Pérez et al. 2014). Madeira, officially a Portuguese territory, and the Canary islands, governed by Spain, are part of the Macaronesian archipelago, along with the Azores and Cape Verde islands. The Macaronesia region consists of small islands scattered across the North Atlantic, most of volcanic origin, hosting more than 2.1 million people (Cropper and Hanna 2014; Karnauskas et al. 2016). These islands provide crucial ecosystem services due to their unique landscapes and offer strategic and economic benefits to their respective countries. They have a subtropical to semi-desert climate dominated by the northeasterly trade winds (Pérez et al. 2014), the Atlantic ocean currents and the Azores high-pressure system (Cropper and Hanna 2014), and by the North Atlantic Oscillation (NAO). Cropper and Hanna (2014) and Herrera et al. (2001) suggest that the total precipitation in the Canary islands and Madeira is related to the NAO index, which increases the strength of the trade winds, enhancing orographically-induced rainfall on the windward slopes (Espinosa and Portela 2020). Moreover, the highly variable topography creates a variety of microclimates on each island, each forming a highly varied distribution of temperature and precipitation patterns (Fragoso et al. 2012). In recent years, these islands have been increasingly subject to precipitation-related natural catastrophes, especially flash floods and landslides, and the increasing occurrence of fire due to a combination of high temperatures, low humidity, low rainfall and often high winds (Carrillo et al. 2022). In Madeira, flash floods usually turn into uncontrollable flows (Fragoso et al. 2012): remarkable events hit Madeira on 20 February 2010 and 5–6 March 2023. Since the Canary and Madeira islands host many natural and cultural tourist attractions, a robust assessment of the behavior of heavy precipitation and extreme temperature events is of crucial interest not only to scientists and policy makers, but also to stakeholders in the local authorities, climate services and tourism industry. In this perspective, to better understand the role of climate change in natural hazards and the impact on ecosystems and infrastructures, simulations of climate models have emerged as fundamental tools of analysis (Benevolenza and DeRigne 2019; Adinolfi et al. 2021; Beaugrand 2009). The spatial resolution of General Circulation Models (GCMs) has proven to describe the processes occurring on continental and intercontinental scales. Nonetheless, many studies in the last decade (Ban et al. 2014, Leutwyler et al. 2017, Ban et al. 2021, Adinolfi et al. 2023 and Fosser et al. 2024) have shown the benefits of dynamically downscaling fine-scale processes at km-scale (4 km or less). Models with such a resolution are able to explicitly resolve deep convection, which allows to switch off the respective parameterization. These km-scale models better represent complex topography and associated boundary layer processes, which tend to improve the simulation of precipitation (Ban et al. 2021; Fosser et al. 2024), as well as the 2-meter air temperature and wind components (Prein et al. 2015, Sangelantoni et al. 2024 and Molina et al. 2024). The promising results obtained by Ban et al. (2021) and Pichelli et al. (2021) for the Alpine region reinforced the need to expand the analysis of km-scale model performances by bridging the gap between inland European (EU) territories and outermost region, as is the case for the Canary and Madeira islands. Moreover, such small islands are a challenging environment for climate models due to their limited extension, sharp gradients of climatological characteristics (i.e. the presence of microclimates), fine-scale processes (i.e. orographically-induced rainfall), gravity wave propagation, land-sea breezes, deep moist convection and complex surface heterogeneities (Lucas-Picher et al. 2021). Km-scale models could provide new insights in island climates that are not solely explained by increased resolution but also by a better representation of such fine-scale processes. Nonetheless, modeling studies at km scales spanning climate-relevant periods (over 10 years) are rare due to the computational burden, especially over the Macaronesian islands. Previous studies on the Canary Islands have focused on present-day analyses (Pérez et al. 2014; Prein et al. 2015). Future projection studies were conducted by Expósito et al. (2015) and Pérez et al. (2022). Expósito et al. (2015), using the pseudo-global warming technique, showed that, at 5 km horizontal resolution, there is a clear dependence of temperature increase with height and a positive change in diurnal temperature range, mainly due to a reduction in soil moisture as a consequence of a decrease in precipitation. Pérez et al. (2022) used dynamical downscaling with the WRF model over Canary islands at a 3 km resolution until the end of the century, under RCP 4.5 and 8.5 scenarios, finding that, despite some biases, the models showed good skill in simulating extreme temperature indices, and that temperature extremes will increase significantly, driven by decreased soil moisture and altered synoptic patterns. Over Madeira, Gao et al. (2023) studied vortex shedding over the present-day 10-year period of the COSMO-crCLIM simulations (also used in this paper and described in Sect. 2). They investigated the representation of the inversion height, and properties of vortex streets regarding shedding period and the structure of the vortices. Vortex shedding was found to have a pronounced annual cycle with an increasing vortex-shedding rate from April to August and a sudden decrease in September. The flow splitting and vortex shedding are found to be essential elements of the climate of mountainous islands in the subtropics, but not resolved in low-resolution global climate models. Moreover, they noticed an improvement in the simulation of hourly precipitation over the Madeira islands compared to convection-parameterized regional climate models. Other studies based on km-scale climate projections run by single models (Bony et al. 2006; Carrillo et al. 2023) investigated the processes related to the ocean-land interface or the orientation of slopes, upwind or downwind of the prevailing trade winds, also having a significant influence on drought events. The state-of-the-art climate knowledge in this region is mainly based on single regional climate model simulations, as, due to their geographical position, the Canary islands and Madeira, although governed by EU countries, are not included in coordinated initiatives of the World Climate Research Programme (WCRP) (Jacob et al. 2020), such as the ensemble climate simulations over the EURO-CORDEX domain (Giorgi et al. 2019). So, on the one hand, the Canary and Madeira islands pose a challenge regarding climate simulations due to their complex topography and need more reliable, higher-confidence projections of changes in all relevant climate hazards to understand and adapt to the risks they pose to human societies and ecosystems (Evans et al. 2024). On the other hand, although representing assets for the EU countries due to their strategic and economic benefits, they are excluded from regional climate ensemble simulations initiatives. These are the reasons behind the motivation of the Horizon-2020 European Climate Prediction system project (EUCP, Hewitt and Lowe 2018) to provide climate projections at km-scale not only over the main continent, but also over the EU outermost regions. Indeed, providing km-scale climate projections covering a period of (at least) 10 years at a grid spacing of 2–3 km was among the main goals of the project. A coordinated multi-model ensemble was built over a common domain of the Alpine region, also in the framework of the CORDEX Flagship Pilot Studies (Coppola et al. 2020) on Convective phenomena (CORDEX FPS-CONV). However, over the EU outermost regions, there was no proper coordination due to time and resource constraints. With such consideration, the ETH Zürich (ETH) in Switzerland, and the Euro-Mediterranean Center on Climate Change (CMCC) in Italy have successfully performed km-scale simulations over the Madeira and Canary islands domain, even if they used different modelling approaches (Sect. 2). Although it is not possible to provide reliable ensemble-like climate projections due to the lack of harmonized experiments, this study explores challenges posed by uncoordinated simulation efforts in view to improve future planned downscaling initiatives. Moreover, the simulations used in this study aim to enhance state-of-the-art knowledge of the microclimate of the Macaronesian islands and the analyses explicitly investigate the climate projections at km-scale resolutions, providing support for urgent adaptation and mitigation decisions. The novelties of the study rely on: (1) the inter-comparison analyses of two kilometer-scale models with available observations as well as on the provision of km-scale simulations under present and future climate conditions, (2) promote the availability of such high-resolution climate information, particularly useful to local climate services, policy makers and stakeholders for adaptation purposes trying to bridge the gap between climate projection providers and users, (3) provide insight into some scientific questions that are still unexplored due to lack of high-resolution gridded observations and high-resolution climate simulations over these territories, as the distribution of temperature and precipitation (mean and extremes) in the km-scale versus coarser resolution models against available observations and reanalyses, as well as the changes in temperature and precipitation as projected by different km-scale modelling approaches. Moreover, the role of large-scale driving conditions in shaping the km-scale projections is also considered. The paper is structured as follows: the models, data and methods are presented in Sect. 2, the results are presented in Sect. 3, and the conclusions are enumerated in Sect. 4.

## 2 Materials and methods

### 2.1 Models description

The regional climate simulations presented here are based on the COSMO-CLM model used by CMCC, and the COSMO-crCLIM model run by ETH. COSMO-CLM and COSMO-crCLIM belong to the same regional climate model family, the COnsortium for Small-scale MOdeling (COSMO, http://www.cosmo-model.org/, https://www.clm-community.eu/), with several differences highlighted below. COSMO is a non-hydrostatic limited-area model that is specifically designed for simulations on meso-$\beta$ to meso-$\gamma$ scales (Steppeler et al. 2003), i.e. on a spatial extent between 2 and 200 km, and describes fully compressible flow in a moist atmosphere using finite difference methods on a structured grid (Rockel et al. 2008). Horizontal advection is simulated using a fifth-order upwind scheme and vertical advection by the means of an implicit Crank-Nicholson scheme (Baldauf et al. 2011). Additionally, the one-dimensional Bott scheme is used for the multidimensional advection of scalar fields (Bott 1989). The numerical computation of the thermodynamical equations is performed on a three-dimensional Arakawa-C grid (Arakawa and Lamb 1977), using rotated geographical and terrain-following height coordinates (Doms and Baldauf 2021). Furthermore, the model uses a split-explicit third-order Runge–Kutta time-stepping scheme (Wicker and Skamarock 2002). For the representation of unresolved processes, the following physical parameterization schemes are used (Baldauf et al. 2011): a radiative transfer scheme based on the $\delta$-two-stream approach (Ritter and Geleyn 1992), a single-moment bulk cloud-microphysics scheme with five species (cloud water, cloud ice, rain, snow and graupel) (Reinhardt and Seifert 2006), a turbulence scheme using a turbulent kinetic energy closure for the surface and the planetary boundary layer (Raschendorfer 2021), and a multi-layer soil model (TERRA-ML) with a total soil depth of 15.24 m (Heise et al. 2006). Depending on horizontal resolution, sub-grid convection is parameterized using an adapted version of the Tiedtke mass-flux scheme with a moisture convergence closure (Tiedtke 1989). Aerosols are imposed using the AeroCom climatology (Kinne et al. 2006).

COSMO-crCLIM is able to run on Graphics Processing Units (GPU) (Fuhrer et al. 2014, 2018), which enables simulations at higher horizontal resolution within acceptable wall-clock timescales (Schär et al. 2020). Besides reducing the simulation runtime, the GPU implementation does not significantly affect the model behavior, as has been shown by Zeman and Schär (2022). COSMO-crCLIM is based on COSMO model version 5.0.9. Simulations on GPUs are executed up to 3.6 times faster than simulations running on the same number of multicore CPUs (Leutwyler et al. 2017). Moreover, COSMO-crCLIM uses the groundwater scheme developed by Schlemmer et al. (2018). Other adjustments include changing the upper-level damping to only relax the vertical velocity instead of all dynamical fields (Klemp et al. 2008). The COSMO-CLM kilometer-scale simulation is based on the model version 5.0.9 associated with the interpolator version int2lm_2.00_clm4 while the coarse-resolution simulations is based on version 4.21.2. The COSMO-CLM simulations were performed on the supercomputer facility available at CMCC.

## 2.2 Simulations setups

As the development of these simulations was not originally planned and coordinated within the EUCP project, the two models use different simulation setups, summarized in Table 1.

### 2.2.1 COSMO-CLM setup

COSMO-CLM uses a three-step one-way nesting approach using a resolution of 0.44° (~50 km horizontal grid spacing) and 0.22° (~25 km) for the first and second nests, respectively, over the Middle-East-North-Africa (MENA) CORDEX domain (Bucchignani et al. 2018, 2016; Zittis et al. 2021), and 0.0275° (~3 km) for the third nest over the analysis domain. This simulation strategy allows to capitalize existing coarse simulations available at CMCC, developed in the context of the CORDEX-MENA initiative. Then, the 0.22° simulations were dynamically downscaled with COSMO-CLM over the Macaronesian domain in the context of the EUCP project, using the same strategy as for the Alpine domain (Ban et al. 2021; Pichelli et al. 2021).

In the two coarse-resolution (50 and 25 km) simulations, convection is fully parameterized as detailed in Sect. 2.1. In the high-resolution (3 km) simulations, only shallow convection is parameterized, while parameterization is switched off for deep convection to allow the model to simulate deep convective processes explicitly (Ban et al. 2021). A one-year period is considered as spinup for the 3 km-scale simulations. COSMO-CLIM uses the so-called *time-slice* approach (Lucas-Picher et al. 2021) running continuous simulations for, at least, 10-year long periods, due to the high computational costs (Giorgi et al. 2009), aligning with the approach used over the Alpine domain (Ban et al. 2021; Pichelli et al. 2021; Fosser et al. 2024). To assess future changes, the CMCC km-scale climate simulation performed over the historical period is compared to the simulation of the same length, but in the future, where greenhouse gas concentrations and boundary conditions are modified according to the RCP8.5 scenario (Riahi et al. 2011).

### 2.2.2 COSMO-crCLIM setup

COSMO-crCLIM uses a two-step one-way nesting approach with a resolution of 0.11° (~12 km horizontal grid spacing), and 0.01° (~1 km) for the second nest over the analysis domain. In the coarse-resolution (12 km) simulations, both deep and shallow convection are parameterized as detailed in Sect. 2.1. In the high-resolution (1 km) simulations,

**Table 1** Key numerical features of the two kilometer-scale simulations: COSMO-CLM performed by CMCC and COSMO-crCLIM performed by ETH

| Model | Nesting | Approach | Forcing | Experiments |
|---|---|---|---|---|
| CMCC - COSMO-CLM v5.09 | Three-step one-way nesting:<br>0.44° (~50 km)<br>0.22° (~25 km)<br>0.0275° (~3 km) | Time-slice experiment GCM-driven | EC-EARTH r12i1p1 (historical and RCP8.5) | Present-day: 1996–2005<br>Future: 2090–2099 |
| ETH - COSMO-crCLIM | Two-step one-way nesting:<br>0.11° (~12 km)<br>0.01° (~1.1 km) | PGW approach: reanalysis-driven (ERA-Interim) | MPI-ESM-LR r1i1p1 RCP8.5 | Present-day: 2006–2015<br>Future: Present-day plus PGW signal from GCM (monthly mean of the difference 2070–2099 versus 1970–1999) |

convection parameterization is switched off for both shallow and deep convection, allowing fully explicit simulations of convective processes.

The driving data used for the coarse-resolution present-day simulation is based on the 6-hourly ERA-Interim reanalysis from the European Center for Medium-Range Weather Forecast [60] for the period 01/2000–12/2015. This period includes a period of five years to allow for soil moisture spin-up. The high-resolution simulations are then computed for the period 11/2005–12/2015, which includes a soil moisture spinup period of two months.

COSMO-crCLIM uses the so-called *pseudo-global warming* (PGW) approach (Brogli et al. 2023). PGW offers the possibility to address simulation uncertainties related to GCM biases (Lucas-Picher et al. 2021). In the PGW approach, the boundary conditions for future climate simulations come from a reanalysis that is perturbed by future changes of the 3D atmospheric conditions taken from a GCM or an ensemble of GCMs (Schär et al. 1996; Expósito et al. 2015; Brogli et al. 2019). The sequence of synoptic-scale weather events and the large-scale atmospheric circulation are therefore preserved in future climate simulations (Lucas-Picher et al. 2021), but individual events are modulated by thermodynamics and dynamics changes as simulated by the high-resolution models. With such a method, uncertainties related to internal variability can be reduced, even when using a relatively short period of 10 years (Kawase et al. 2008). It also reduces the number of simulations required to conduct climate change analysis because no historical climate simulation is needed. A detailed discussion of advantages and disadvantages of the PGW methodology can be found in (Brogli et al. 2023). They also provide a quantitative comparison between conventional and PGW downscaling at a resolution of 50 km. To build the future climate simulation, ETH uses the climate change signal of the Max-Planck Institute MPI-ESM-LR CMIP5 Earth System Model r1i1p1 (Giorgetta et al. 2013), under the RCP8.5 scenario (Riahi et al. 2011). The above explanation of the PGW approach suggests an increased robustness provided by this method when several GCMs are involved. However, it needs to be stated that the COSMO-crCLIM simulation is based on an older version of the PGW approach that focuses on the signal of one GCM instead of a GCM ensemble mean, as was done by Brogli et al. (2023) with the same model for their analysis of precipitation indices. The PGW signal was computed using the monthly mean of the difference between 2070–2099 and 1970–1999. This signal was applied to the 2006–2015 present-day simulation. The spinup periods are individually chosen by ETH and CMCC based on their own expertise and experiences over different domains. Recent studies as Jerez et al. (2020) and Lavin-Gullon et al. (2023) suggest a minimal spin-up period of 1-year, although longer spin-up times could be considered in order to be on the safe side of soil spin-up, depending on the region and deep convective events.

## 2.3 Computational domains

Figure 1 shows (right panels) the islands of Madeira, Tenerife and Fuerteventura as represented by each model

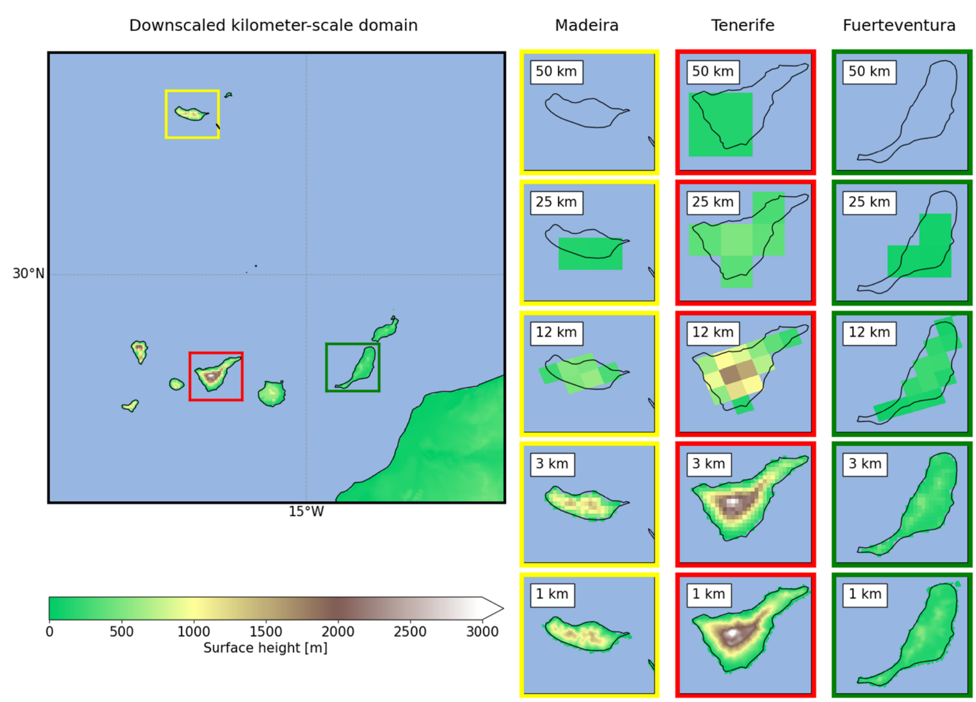


**Fig. 1** Topography (in meter) of the investigated simulation domain and individual islands. (Left) Common km-scale simulation domain over the Macaronesian islands (here shown at 3 km grid spacing). (Right) The three islands analyzed in this study: Madeira, Tenerife and Fuerteventura (from left to right) and the different model resolutions: CMCC at 50 and 25 km, ETH at 12 km, CMCC at 3 km and ETH at 1 km grid spacing (from top to bottom). Orography is shown for grid cells with a land fraction above 50%, while grid cells with a land fraction below 50% are coloured in blue

simulation used in this study, so at 50, 25, 12, 3 and 1 km grid spacing (from top to bottom). It emerges a detailed orography depicted at higher resolutions over the islands compared to lower resolutions. Madeira and Fuerteventura are not even represented in a 50 km model, while Tenerife is covered by only one grid point with a flat orography. All islands are represented at 25 km grid spacing, although with a flat orography. It is only from 12 km grid spacing onward that differences in orography start to emerge, particularly in Tenerife, where the two kilometer-scale resolution simulations (3 and 1 km grid spacings) adequately capture the peak elevation of more than 3500 m a.s.l. (Fig. 1, two bottom right panels). Fuerteventura is much flatter than Madeira and Tenerife, and the island's orography is already well captured at 12 km grid spacing, yet the km-scale representations show detailed orographic variations not seen at coarser resolutions.

The left panel of Fig. 1 represents the topography of the whole km-scale simulation domain, common for both simulations. The computational domain simulated by CMCC with COSMO-CLM (hereafter referred to as CMCC) at 3 km grid spacing (Lon = 20°W–11°W; Lat = 25.5°N–34.4°N) consists of 327 × 323 grid points, 65 vertical levels and 7 soil layers. The analysis domain is obtained by discarding the relaxation zone from the computational domain (23 points for each border). The computational domain simulated by ETH with COSMO-crCLIM (hereafter referred to as ETH) at 1 km grid spacing (Lon = 20.1°W–13.5°W; Lat = 23.1°N–38.8°N) consists of 1000 × 1000 grid points, 60 vertical levels and 9 soil layers. The analysis domain is obtained by discarding the relaxation zone from the computational domain (30 points for each border).

## 2.4 Validation data

In order to evaluate the reliability of the simulations, both CMCC and ETH simulations have been compared to available observational and reanalysis products for the present-day period covered by the simulations: 1996–2005 for CMCC and 2006–2015 for ETH. Reanalysis products, gridded observations (available over the Spanish islands) and station data are considered for evaluating simulated precipitation and temperature patterns. Other satellite products, such as GPM IMERG that provides hourly precipitation at 0.1° × 0.1° (or roughly 10 km × 10 km) grid spacing, have been considered but show spurious behaviour over the islands that need further investigation and evaluation (not shown). They are therefore not included in this study.

### 2.4.1 ERA5 reanalysis

ERA5 reanalysis (Hersbach et al. 2020) are produced by the Copernicus Climate Change Service (C3S) at the European Centre for Medium-Range Weather Forecasts (ECMWF). ERA5 is the fifth generation atmospheric reanalysis of the global climate covering the period from January 1940 to present, at hourly intervals. In this study, we use hourly 850-hPa wind, sea level pressure, 2-meter temperature, precipitation and sea surface temperature (SST) data for the period 1996–2015, which corresponds to the continuous 20-year period covered by the two kilometer-scale model simulations. The data use a horizontal resolution of 0.25° (about 30 km grid spacing) and 137 vertical levels from the surface up to a height of 80 km.

### 2.4.2 UERRA reanalysis

UERRA is a reanalysis that provides estimations of the climate in Europe for the period 1961–2019 (Gustafsson et al. 2001; Uncertainties in Ensembles of Regional Re-Analyses 2017). It consists of two reanalyses: UERRA-HARMONIE and MESCAN-SURFEX. UERRA-HARMONIE is a regional reanalysis over Europe based on a 3-dimensional variational data assimilation system. It is available at ~11 km grid spacing. In addition to observations in the model domain, it assimilates along the lateral borders data from ERA40 (until the end of 1978) and ERA-Interim (from 1979). MESCAN-SURFEX is a complementary surface analysis system forced by the UERRA-HARMONIE reanalysis. Using the Optimal Interpolation method, it provides daily accumulated precipitation and six-hourly air temperature and relative humidity at two meters above the model topography at ~5.5 km grid spacing. For this study, we use 6-hourly 850-hPa wind, sea level pressure and SST at 11 km grid spacing and daily precipitation and 6-hourly 2-m air temperature at 5.5 km grid spacing over the period 1996–2015 (Copernicus Climate Change Service, C.D.S., 2019).

### 2.4.3 NOAA sea surface temperature

Daily SST data were retrieved from the National Oceanic and Atmospheric Administration Optimum Interpolation Sea Surface Temperature database at a resolution of 0.25° (NOAA OISST v2; https://www.ncdc.noaa.gov/oisst).

### 2.4.4 Observations from gridded and weather station data

The weather station hourly precipitation data are operated by the Agencia Estatal de Meteorología (AEMET) for Tenerife and Fuerteventura and by the Instituto Português do Mar e da Atmosfera (IPMA) and the Delegação Regional da Madeira do IPMA for Madeira.

The rain gauges over Madeira provide data every 10 min, but the measurements have been aggregated to hourly data to be consistent with the model output frequency and the station data over the Canary Islands. Figure 2 provides an overview of the rain gauge locations and the number of years with available data. All islands are sufficiently covered by rain gauges, although over Fuerteventura the coverage is relatively sparse with only six stations and only one station has more than 10 years of hourly data over the period 1996–2020.

The AEMET provides high resolution (2.5 km) gridded observational precipitation and temperature datasets for Canary islands at daily and subdaily scale (Peral García et al. 2017).

## 2.5 Indices and statistics

The characteristics of temperature and precipitation over the islands of Madeira, Tenerife and Fuerteventura are investigated at seasonal, daily and hourly scales. Specifically, the indices assumed for the statistical measures of precipitation are mean precipitation, wet-hour frequency, wet-hour intensity, and heavy precipitation analysis in terms of 99.9th percentile of hourly data to estimate extreme precipitation events. A wet-hour is defined as an hour with precipitation ≥ 0.1 mm/h, while the extreme precipitation events are investigated through the amount of hourly precipitation above the 99.9th percentile computed from all data (wet and dry events), according to (Ban et al. 2021). The daily maximum temperature (Tmax) and mean temperature are used as temperature indices. All indices are computed per season (DJF = December–January–February; MAM = March–April–May; JJA = June–July–August; SON = September–October–November), then averaged over the analysis period. For statistics concerning the specific islands, only land grid cells are considered in the analyses. For the representation of the diurnal cycle of mean precipitation, the hourly precipitation is then averaged over the islands' land fraction. The statistics of hourly precipitation and daily temperature are also investigated using box plot representations, looking for differences in the statistical spatial distributions. For box plots, the indices are first averaged seasonally. Then, the seasonal mean index over each island land fraction is represented as follows: the halfway mark of the box plots indicates the median, and the bottom and top edges of the box indicate the 25th and 75th percentiles, respectively. The whiskers are defined as ± 1.5 times the interquartile range (IQR). With such a representation, the box plots therefore synthesize the results of the spatial maps and allow an immediate comparison between models. To assess the climate projection signals, the differences (Δ) between the future and present-day time slices of the aforementioned indices are computed. Specifically, for the CMCC model, the present-day period is 1996–2005 and the future period is 2090–2099, and for the ETH model, the present-day period is 2006–2015 and the future period is 2106–2115. To determine the statistical significance (alpha = 0.05) of the climate projections, a non-parametric Mann–Whitney U test (Mann and Whitney 1947) able to assess the significance of the changes of two series and suitable for non-normally distributed data, is used. A correction to reduce the amount of false positives (FDR) and overcome the overrating of significant changes (Wilks 2016), derived according to the formulation presented in Benjamini and Hochberg (1995), is also applied. The tests run over the 10-year period simulations run by CMCC and ETH, just considering inland grid nodes over the islands, and the statistics as mean, median and variance are calculated for historical and future series. The Mann–Whitney U test yields a p-value: a p-value below the significance level alpha indicates significant changes. The inland grid nodes where the statistical significance of changes (p-value) is greater than 0.05 are stippled in the spatial analyses. Spatial analyses are shown over Madeira for present-day climate (Sect. 3.2), over Tenerife and Madeira for future climate (Sect. 3.3), while maps and analyses for the other islands are included in the supplementary material.

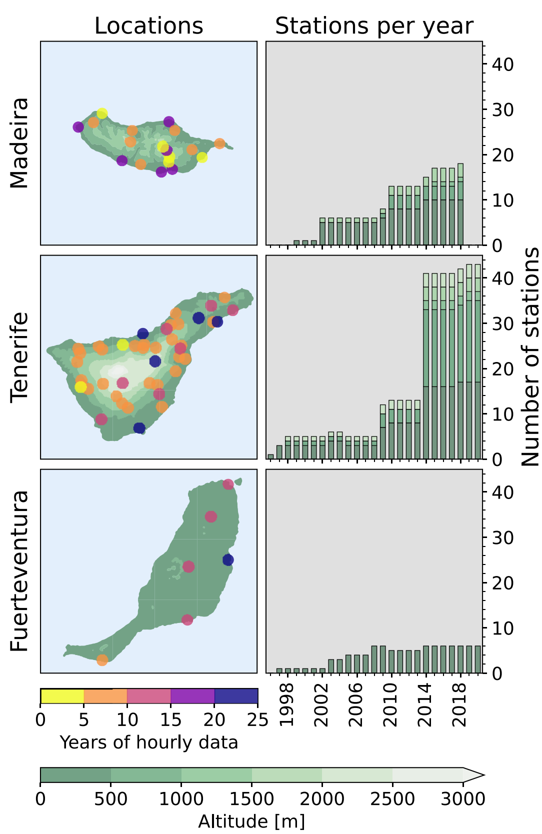


**Fig. 2** Overview of rain gauge locations and years with hourly precipitation data that were used for validation

## 3 Results

The section is composed of three subsections presenting the evaluation of the large-scale climate conditions over the Macaronesian domain against available reanalyses and observations, the assessment of current climate km-scale simulations of precipitation and temperature over the three selected islands, and their climate projection signals.

### 3.1 Evaluation of large-scale climate conditions in the Macaronesian domain

Figure 3 shows the large-scale climate conditions in autumn (SON) as simulated by the CMCC and ETH models at intermediate resolutions (25 and 12 km grid spacings, respectively) over the whole domain against reanalysis. From left to right, Fig. 3 gives a synoptic perspective on the mean 850-hPa wind along with sea level pressure, 2-meter temperature, precipitation regimes and SST over the extended Macaronesian domain. As the regional climate models neglect the interactive feedback of the atmosphere and the ocean, examining the synoptic scale of the atmosphere is supported by SST to provide a comprehensive picture of the real climate system, especially over such small islands and coastal territories. The first and second rows depict the signals of ERA5 and UERRA reanalyses, while the third and fourth rows show the variables as simulated by CMCC and ETH at intermediate resolutions. The signal of the two reanalyses was calculated over the period 1996–2015, which covers the continuous 20-year time period of the CMCC (1996–2005) and ETH (2006–2015) present-day periods. The geographical extent of each dataset was adjusted to the domain of the ETH intermediate simulation. The two reanalyses, ERA5 and UERRA, show very similar results in temperature, SST and precipitation, although there are some differences along the coast of Africa probably due to the higher resolution of UERRA compared to ERA5. On the opposite, ERA5 underestimates the 850 hPa wind with respect to UERRA. When compared to the two models, it emerges that the ETH simulation is closer to UERRA reanalysis than CMCC. This could be explained by the differences in the model setups, indeed ETH is driven by ERA Interim reanalysis, while CMCC is driven by the EC-EARTH GCM (Sect. 2.2). In the supplementary material, Figure A.1 shows the signal of 2-meter temperature over the analysis domain as represented by the EC-EARTH and ERA Interim, with a uniform colder behaviour of EC-EARTH GCM with respect to ERA Interim. The SST over the Macaronesian area, represented in the last column of Fig. 3, undergoes small spatial

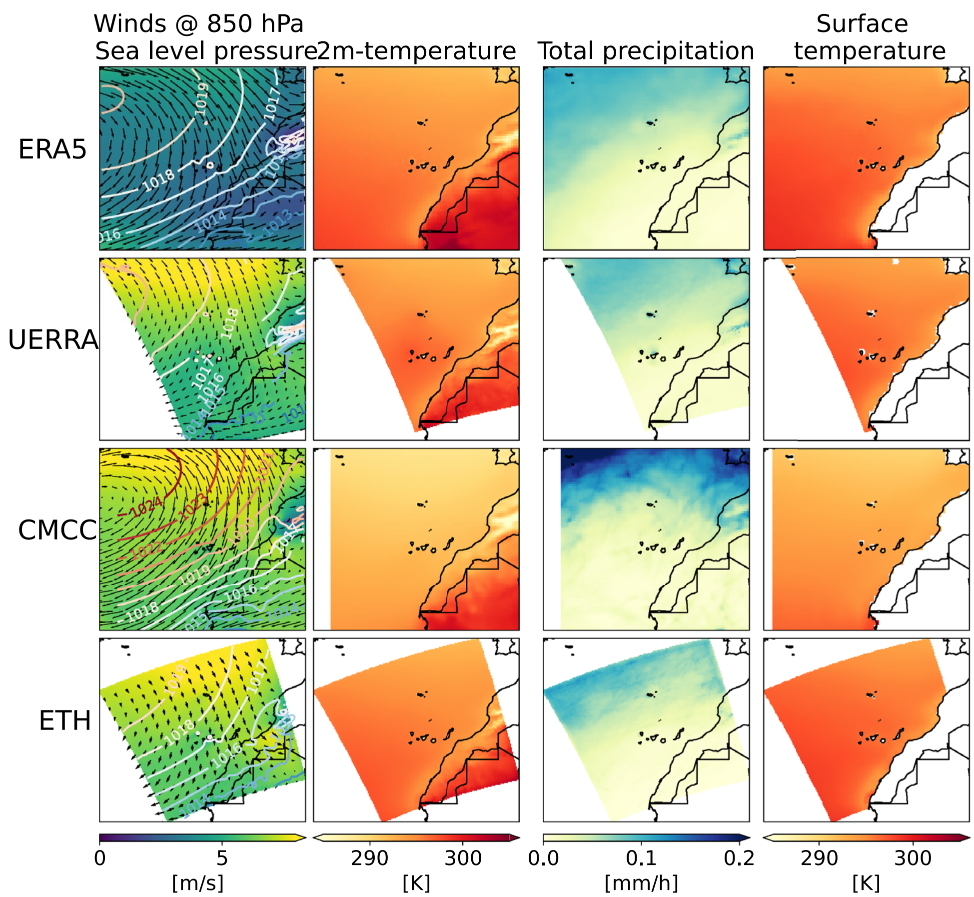


**Fig. 3** Large-scale conditions over the Macaronesian domain for the fall season (SON). The panels show, from left to right, the mean wind speed (shading) and wind direction (vectors) at 850 hPa along with the mean sea level pressure (contours), the mean 2-meter air temperature, the mean precipitation, and the sea surface temperature for (from top to bottom) ERA5 and UERRA reanalyses, and the two intermediate simulations of CMCC at 0.22° and ETH at 0.11° resolutions. The time periods considered are 1996–2015 for ERA-5 and UERRA, 1996–2005 for CMCC and 2006–2015 for ETH

variations during the SON period with a mean range of approximately 290–300 K for both reanalysis and models. The spatial patterns show that the warm water mass located in the southwest, gradually reduces towards the northern part of the domain. Thus, models are able to reproduce the Canary upwelling system (as documented in other studies as Varela et al. 2022), also accounting for the coastal temperatures coming from the Western Sahara desert. In Fig. 3, the CMCC model simulates weaker northerly winds, colder near-surface temperature and SST over the Atlantic and the African coast and more mean precipitation in the northern part of the domain. Such differences also occur during the other seasons (Figs. A.2 and A.4) but are smaller in summer (Fig. A.3), when there is a better agreement between CMCC and reanalysis products.

Overall, these results show that the large-scale simulations of the Macaronesian domain, driving the km-scale simulations, are realistic despite some biases of CMCC that are explained by the forcing GCM.

## 3.2 Km-scale present-day simulations of the Macaronesian islands

### 3.2.1 Precipitation

The km-scale current climate simulations of precipitation indices are presented for the islands of Madeira, Tenerife and Fuerteventura. Figure 4 shows precipitation indices for the island of Madeira for the fall season (SON) as simulated by CMCC (3 km grid spacing) and ETH (1 km grid spacing) models compared to IPMA weather station data (top row) and UERRA reanalysis (5 km, second row). Compared to IPMA observations, the UERRA reanalysis underestimates both intensity and p99.9 but reproduces the higher frequency. The UERRA tendency to overestimate precipitation amounts and frequency is well known over other domains (Adinolfi et al. 2023). Both km-scale models generally simulate higher precipitation intensity and extremes (especially ETH model) than the reanalysis product in SON. The CMCC model underestimates precipitation indices compared with IMPA observations. During all seasons (Figs. A.5, A.6 and A.7 in the supplementary material), simulated precipitation intensity and extremes by both CMCC and ETH models are in quite good agreement with IPMA observations, as UERRA reanalysis underestimates the hourly features of precipitation and it overestimates frequencies. Simulated

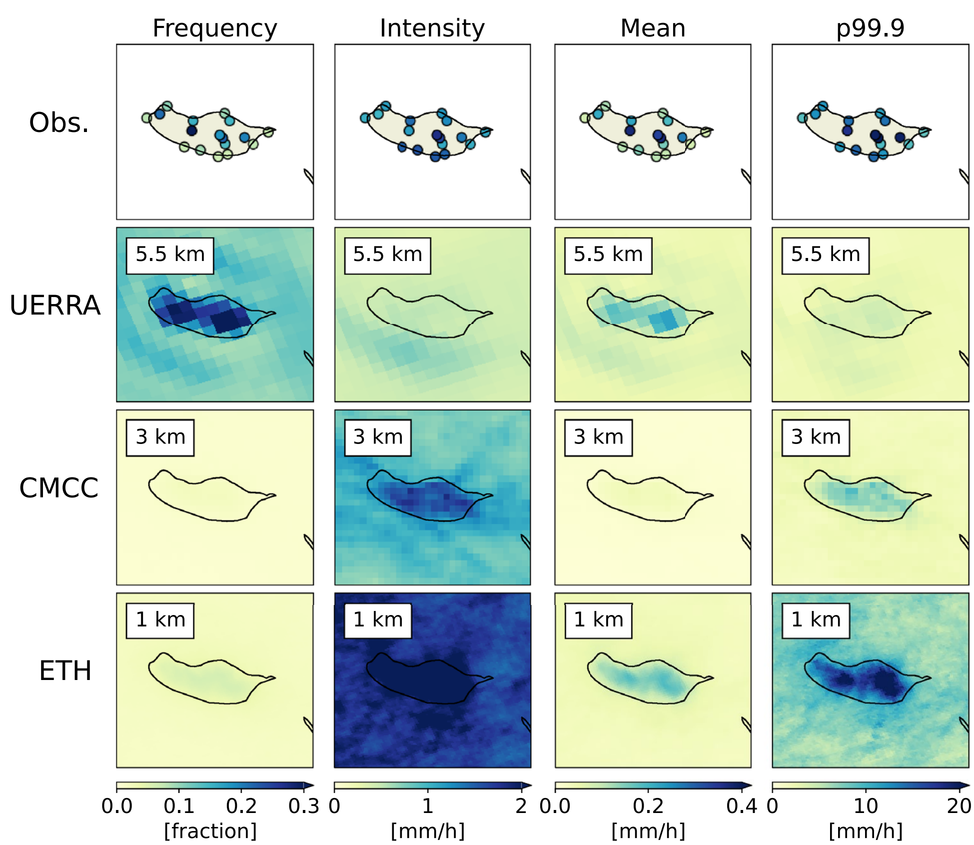


**Fig. 4** Observed and simulated precipitation indices for the island of Madeira for the fall season (SON). (From left to right) precipitation frequency, precipitation intensity, mean precipitation and heavy precipitation (p99.9) as displayed by (from top to bottom) IPMA weather station observations, UERRA reanalysis (5.5 km), CMCC (3 km) and ETH (1 km) models. The indices were calculated over the individual time periods covered by each point station, continuous 20-year present-day time period for UERRA, and over the respective present-day periods for CMCC and ETH. Note the different color scales for the IPMA point observations and UERRA

mean precipitation is higher in SON but lower in DJF, MAM and JJA in the two models compared to reanalysis, although the ETH model tends to be closer than CMCC because of its higher orography-induced precipitation. The models simulate lower precipitation frequency in all seasons compared to reanalysis but in a good agreement with IPMA observations. Both km-scale simulations reveal high precipitation index signals in the interior of the island where mountains are located and smaller signals along the coasts, in agreement with observations. The signals are particularly stronger in the ETH model and attributed to the steeper and higher orography. The spatial relation of precipitation index signals with orography occurs also in other seasons, although in JJA the high precipitation signals are not directly located over orography but along the north-west coast in both models.

The precipitation signals over Tenerife are presented in the supplementary material (Figs. A.8, A.9, A.10 and A.11). The comparison here is against AEMET weather station data (top row) and UERRA reanalysis (5 km, second row). High precipitation index signals over orography and weaker ones along the coasts in all seasons are shown over Tenerife, similar to Madeira. Compared to reanalysis, simulated precipitation intensity and extremes are higher in all seasons except JJA, particularly in the ETH model, being in better agreement with AEMET observations. Simulated mean precipitation is lower in the two models compared to reanalysis and AEMET observations in DJF and SON but is well reproduced in MAM and JJA. The models simulate lower precipitation frequency in all seasons compared to reanalysis and AEMET observations. In DJF, the precipitation signals are not directly located just over the orography, but more diffuse along the island in both models, while the CMCC model captures higher frequency, mean and p99.9 in the northern coast of the island.

The precipitation signals over Fuerteventura are presented in the supplementary material (Figs. A.12, A.13, A.14 and A.15). As for Tenerife, the comparison is against AEMET weather station data (top row) and UERRA reanalysis (5 km, second row). A more uniform precipitation signal is shown over Fuertevenura compared to Madeira and Tenerife, due to its low elevation. The ETH model shows noisy and low precipitation signals in all indices in JJA, where the model is drier than CMCC. Compared to reanalysis, all precipitation indices are higher in all seasons, except in MAM. CMCC model in JJA uniformly overestimates intensity with respect to reanalysis and AEMET observations. ETH model in SON uniformly overestimates frequency with respect to reanalysis and AEMET observations.

Figure 5 summarises the previous results and allows a comparison between observations, UERRA, CMCC and ETH models. Overall, the two models, despite their different resolutions and simulation setups, show differences with observations and UERRA, but quite similar values for all indices over each island and for each season, except in SON over Madeira. In that case, the ETH model particularly simulates very high precipitation mean and extremes attributed to its higher orography (as shown in Fig. 4). Some differences are also observed in precipitation intensity during JJA over Tenerife and Fuerteventura, where the ETH model tends to be particularly dry but occasionally produces peaks of high intensity (up to nearly 15 mm/h). However, these peaks are not captured by the 99.9th percentile values, which remain close to zero. This occurs because the 99.9th percentile threshold for hourly data, which includes dry hours, is probably not sufficient to adequately capture extreme events and even standard precipitation are reproduced as extreme events in these small regions, where wet hours, particularly in JJA, are rare. Therefore, in the box plot, such events appear as outliers. The spatial variability (represented by the distance between the lower and upper buffer of the box plots) in the models is higher in DJF and lower in JJA than in other seasons for all islands and all indices except intensity. From the comparison with observations and UERRA vs the km-scale models, it figures out that the km-scale models generally underestimate frequency but there are improvements in representing the extreme events (p99.9), although some discrepancies during SON.

Figure 6 represents the diurnal cycle of mean precipitation over Madeira, Tenerife, and Fuerteventura for each season as simulated by the km-scale models compared with station data reported in green. The diurnal cycle of the CMCC model is averaged over the period 1996–2005, whereas the diurnal cycle from the ETH model is averaged over the period 2006–2015. The diurnal cycle from the station data is taken as an hourly average of all stations with data in the period 1996–2020 (see Fig. 2 for more details). Generally, all islands experience less mean precipitation in summer than in other seasons. This, in agreement with other studies (Gao et al. 2023), can mostly be attributed to the more northern position of the intertropical convergence zone in summer and its associated dry region from the Hadley circulation. The diurnal cycle shape of precipitation occurrence is not clearly pronounced and quite uniform across the day for all islands, even if, during SON over Tenerife, daytime hours are slightly wetter than nighttime hours. It is worth to note that the y-axis range in Fig. 6 is different for each islands, resulting with Madeira, both from models and observation, as the most rainy island of the three and Fuerteventura as the less rainy of them, during all seasons. Although both km-scale models and observations in Fig. 6 refer to different periods, the models are quite able to simulate the dynamics of the mean precipitation diurnal cycle over each island and in each season, although underestimating mean precipitation values. Indeed, a weak mean precipitation signal is shown in JJA while the highest signal occurs in DJF and SON

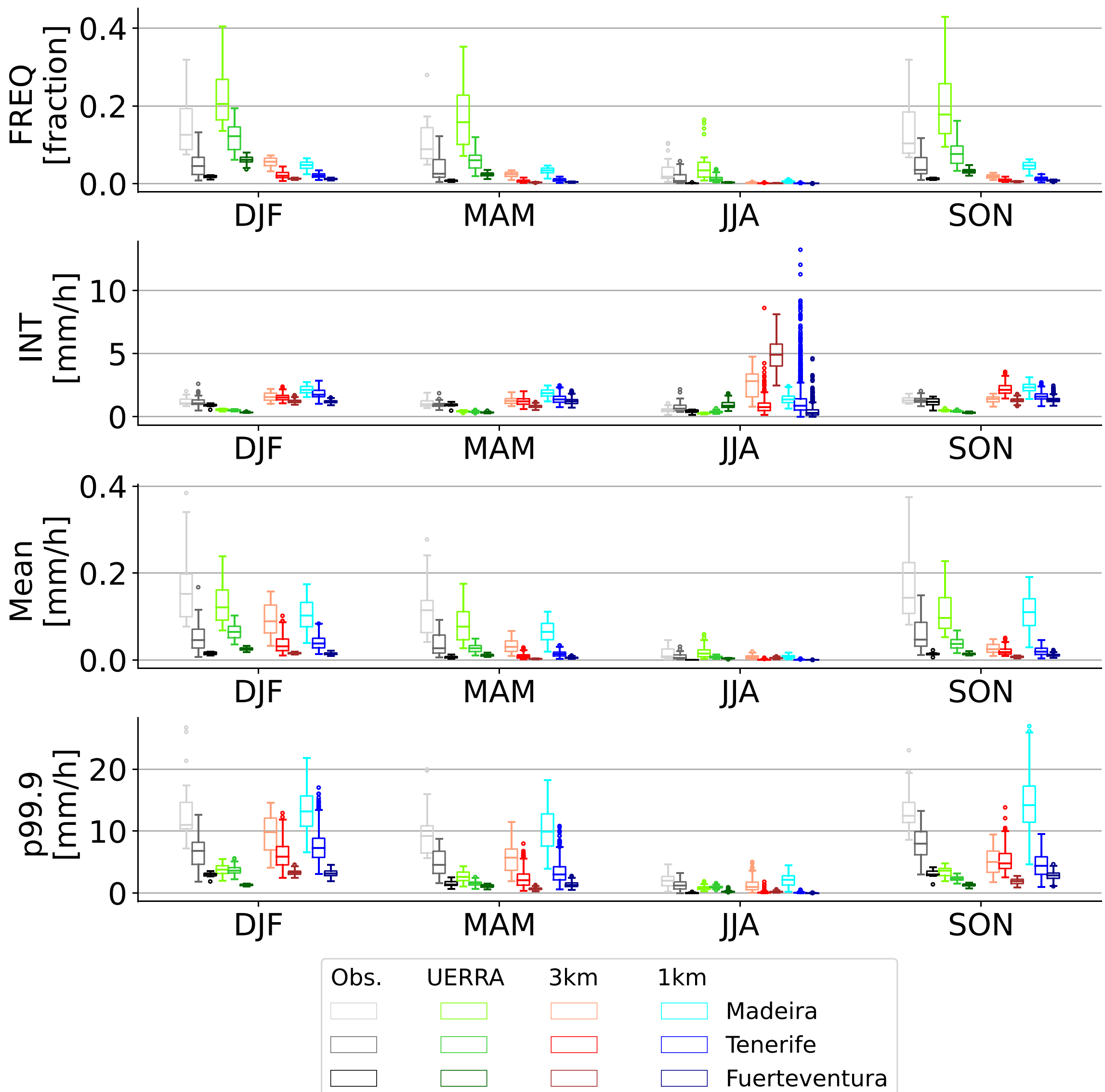


**Fig. 5** Box plots of observed (Obs.), reanalyses (UERRA) and modeled precipitation indices used in the analysis for all seasons. (From top to bottom) precipitation frequency, precipitation intensity, mean precipitation and heavy precipitation as simulated by the CMCC (3 km) and ETH (1 km) models in all seasons for each island. The indices were calculated over the respective present-day periods of each model

over all islands. The occurrence of precipitation during all seasons, following station data, is stronger in Madeira (up to 0.4 mm/h) than in Tenerife (up to 0.07 mm/h) and Fuerteventura (up to 0.03 mm/h). Although some discrepancies appear, the km-scale models reveal their potential ability in the representation of precipitation features, simulating hourly values of precipitation. Nevertheless, unlike for simulations in continental domains, the use of km-scale simulations to improve the representation of the diurnal cycle is less justified simply due to the fact that the diurnal cycle of precipitation is much less distinct due to the small size of the islands.

### 3.2.2 Temperature

The temperature indices for the current climate over the islands of Madeira, Tenerife and Fuerteventura as represented by the UERRA reanalysis and the km-scale CMCC and ETH models are presented in Fig. 7 for the fall season (SON) and in the supplementary material for the other seasons (Figs. A.16, A.17, A.18 and A.19). Compared to reanalysis and observations (available only for the Spanish islands), both models simulate colder 2-meter mean and daily maximum temperatures (Tmax) over all seasons and all islands. The spatial distribution of both mean and max

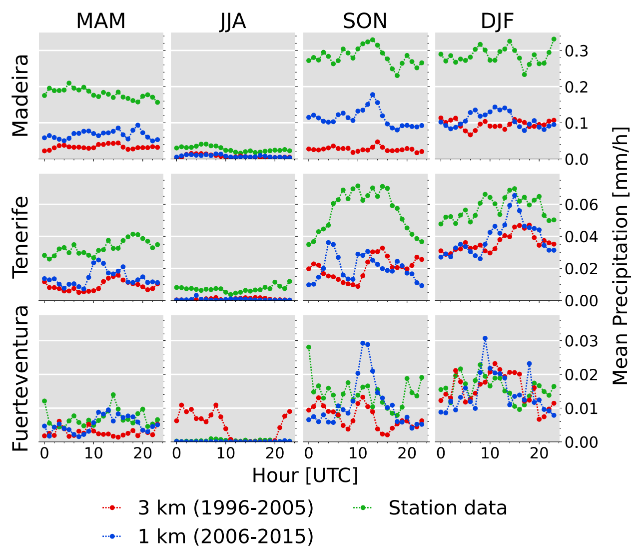


**Fig. 6** Diurnal cycle of mean precipitation for each island and season for station data (green), CMCC 3 km (red) and ETH 1 km (blue) models. Note the different scales for the islands with Fuerteventura and Tenerife getting much less precipitation than Madeira

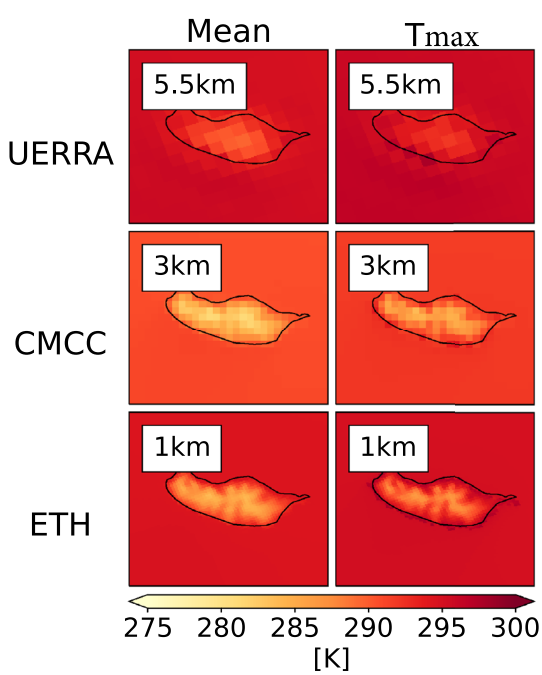


**Fig. 7** 2-meter temperature (mean) and mean of all daily maximum temperatures (Tmax) for the fall season (SON) as represented by (from top to bottom) UERRA reanalyses (5,5 km), CMCC (3 km) and ETH (1 km) models over the island of Madeira. The indices were calculated over the continuous 20-year present-day time period for UERRA and over the respective present-day periods for CMCC and ETH

2-meter temperature depends on the islands topography. Both km-scale simulations reveal lower mean temperatures and Tmax in the interior of the island than in coastal areas, confirming the orography-induced distribution in all seasons over Madeira and Tenerife. The signals over Fuerteventura are more uniform with a good agreement between km-scale simulations. The ETH model simulates higher mean temperature and Tmax than the CMCC model during all seasons and over all islands. This is in agreement with the large-scale temperature signal that highlighted the colder conditions of the CMCC model (Fig. 3 and Figs. A.2, A.3, A.4).

Figure 8 summarises the previous results and allows the comparison among observations, represented by grey boxes, reanalysis, represented by green boxes, CMCC, represented by red boxes, and ETH, represented by blue boxes. The results show consistent values for the temperature indices across the two km-scale models over all islands and in each season. Still, the ETH model tends to be consistently warmer than the CMCC one in all seasons over all islands, and in better agreement with observations and reanalysis. This result is consistent with the large-scale conditions and SST plays a key role influencing the behaviour of the regional models over islands as in a region predominantly occupied by the sea. Indeed, a strictly connection between the SST (Fig. 3 and Figs. A.2, A.3 and A.4 in supplementary material) and mean temperature over islands (Fig. 8) is revealed. In Fig. 8 during SON and JJA, CMCC mean temperature values over all islands are colder than the ETH and UERRA ones, mirroring the SST behaviour (Fig. 3 and Fig. A.3). Due to the uniformity of its flat terrain, Fuerteventura depicts a smaller range of temperature indices with an agreement between CMCC and ETH simulations. Similarly, because of its topography, the range is larger over Tenerife in both models for both mean temperature and Tmax in all seasons but JJA when the range is similar to Madeira. It is worth considering the uncertainties associated with observations over mountains with little measurements and worse quality due to the winds effects that could justify the discrepancies at the lower buffer distribution over Tenerife. Consistently across all islands, the highest mean temperatures and Tmax occur in summer (JJA) and the lowest ones in winter (DJF).

## 3.3 Future climate simulations at km-scale resolution

### 3.3.1 Role of large-scale driving conditions in shaping future km-scale simulations over the Macaronesian islands

Several studies (Giorgi et al. 1999; Rummukainen 2009; Schiermeier 2010; Kerr 2011, 2013; Hall 2014) question the reliability of RCM projections, particularly because they are driven by GCMs, which themselves are unreliable. RCMs would therefore produce more detailed projections, due to their higher resolution, but also noisier projections (the so-called 'garbage in, garbage out' argumentation). Other

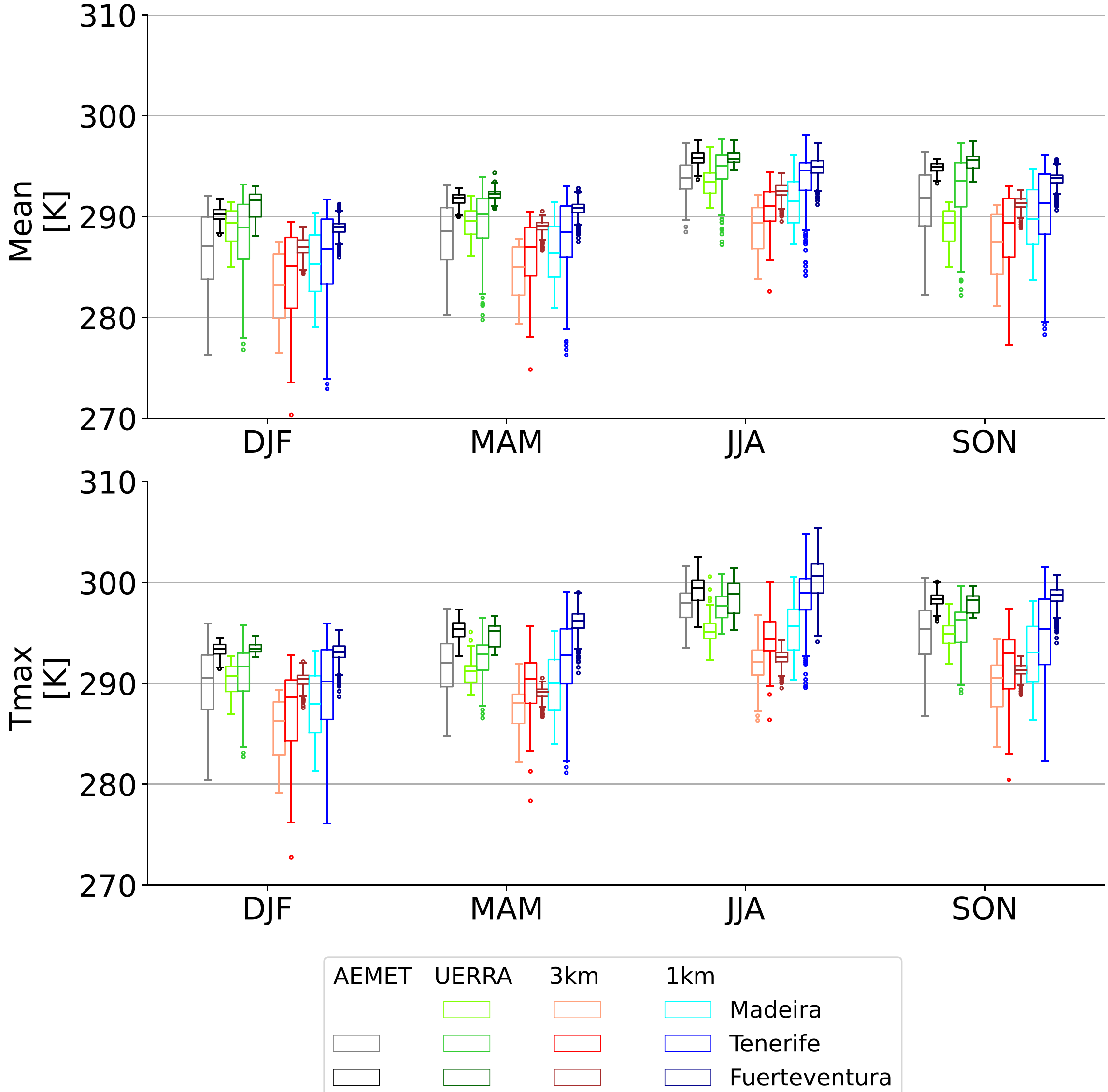


**Fig. 8** Box plots of the gridded (AEMET), reanalyzed (UERRA), and modeled temperature indices used in the analysis for all islands over all seasons. (From top to bottom) 2-meter mean temperature, and Tmax as simulated by the two km-scale models. The box plots with red and blue shadings show results for CMCC (3 km) and ETH (1 km) models, respectively. The indices were calculated over the respective present-day periods of each model. Observation gridded data is absent for Madeira, as AEMET covers only Spanish territories

studies (Sørland et al. 2018) demonstrate that RCMs systematically reduce biases and modify the climate change signals of the driving GCMs, even on scales that are considered well resolved by the driving GCMs. Indeed, while GCMs are tuned to represent the global energy and water balance (to provide global consistency of the simulated climate), RCMs are tuned to represent the regional climate (to provide an optimal representation of the regional processes). In this perspective, the role of driving conditions over the Macaronesian islands is highlighted to find consistency among the GCMs, intermediate simulations and km-scale projections. Specifically, Fig. 9 shows the SST changes in subplot a and changes in 2-meter mean temperature in subplots b and c, as projected by the EC-EARTH GCM (used to drive the CMCC intermediate simulation) and the MPI-ESM-LR (used to drive the ETH intermediate simulation) under the RCP8.5 scenario. The Fig. 9 shows in subplot a that cold water masses along the coast of the Western Sahara desert are projected by both GCMs with SST generally colder (around 2 K) than the NOOA observations, during all seasons. Figure 9 shows (in subplot b) that the EC-EARTH GCM projects warmer temperatures over most of the Macaronesian domain than MPI-ESM, with a temperature difference of around 1−1.5 K between the two GCMs. The temperature difference of EC-EARTH with respect to MPI-ESM GCMs occurs especially along the northwestern coast of Africa,

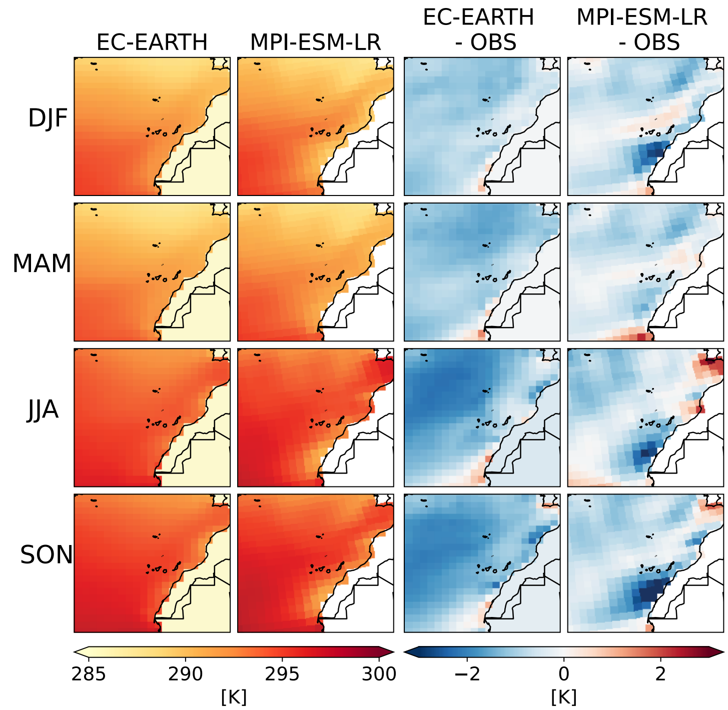


(a) GCM Sea Surface Temperature signals vs. observations: NOAA OISST v2

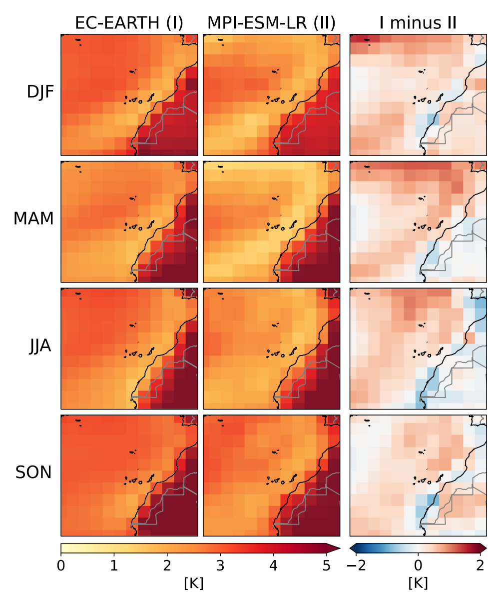


(b) GCMs 2m-temperature future change signals

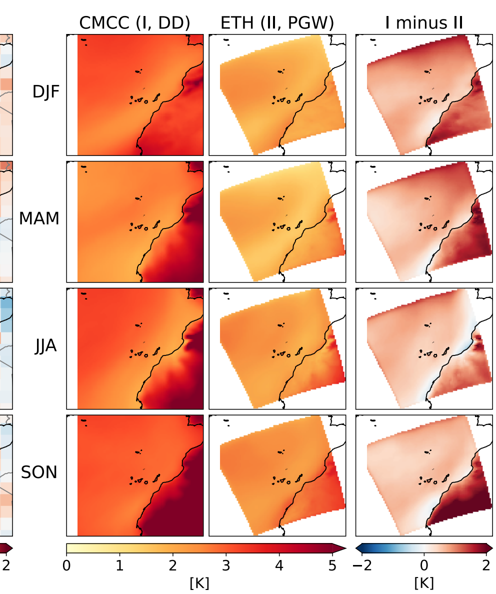


(c) Intermediate 2m-temperature future change signals

**Fig. 9** **a** Mean sea surface temperature in all seasons as simulated by the EC-EARTH GCM, used to drive CMCC, over the CMCC present-day period and by the MPI-ESM-LR, used to drive ETH, over the period 1971–2000, along with the respective bias compared to NOAA OI SST v2 data. **b**, **c** Future changes in 2-meter mean temperature over the entire domain in all seasons. **b** EC-EARTH GCM signals (CMCC future vs present-day period, left column), MPI-ESM-LR GCM signals used to drive ETH (2070–2099 minus 1971–2000, middle column), and differences between the two GCMs (EC-EARTH minus MPI-ESM-LR, right column). The grid of EC-EARTH was remapped onto the MPI-ESM-LR grid. **c** Intermediate projections by CMCC (22 km grid spacing, CMCC future vs present-day period, left column), ETH (12 km, ETH future vs present-day period, middle column), and differences between the two intermediate models (CMCC 22 km minus ETH 12 km, right column). The grid of ETH 12 km was remapped onto the CMCC 22 km grid. DD: Dynamical downscaling; PGW: Pseudo-global warming (refer to Sect. 2.2 for details)

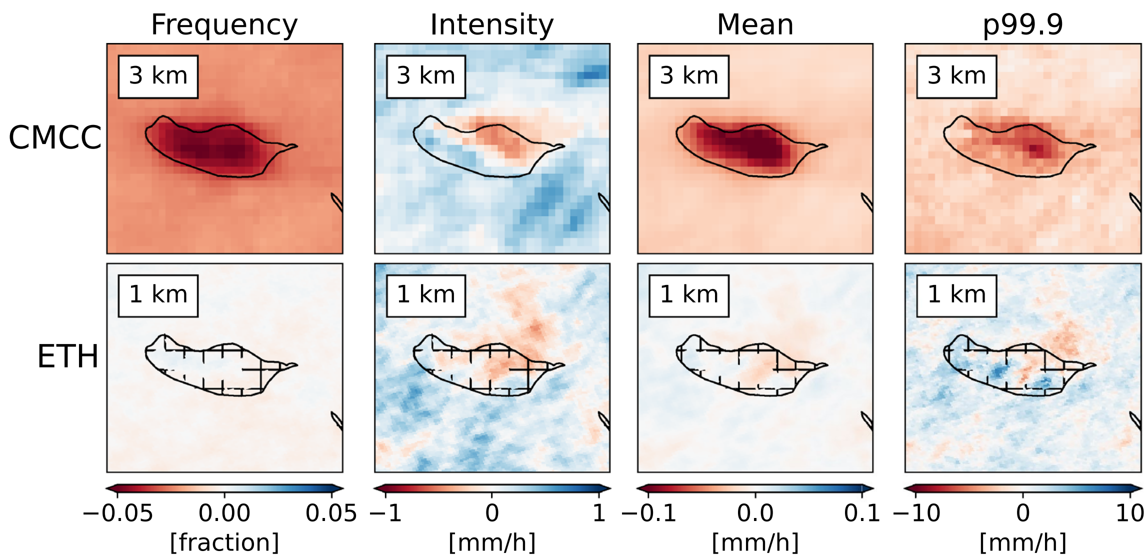


(a) Madeira

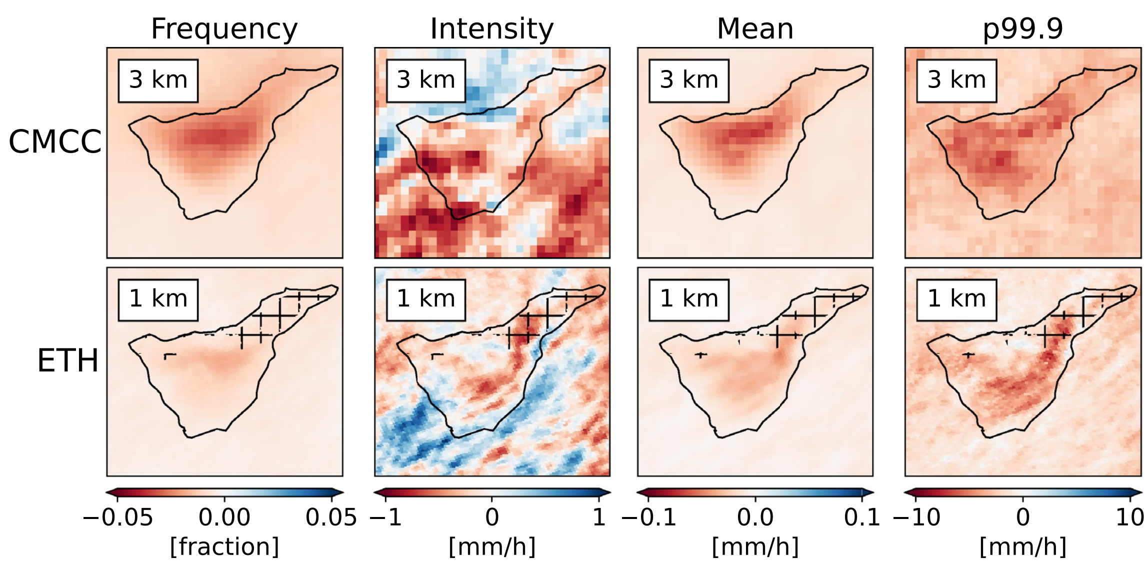


(b) Tenerife

**Fig. 10** Climate change signal of precipitation indices over **a** Madeira and **b** Tenerife for the winter season (DJF). (From left to right) precipitation frequency, precipitation intensity, mean precipitation, and heavy precipitation as projected by the two km-scale models. The differences between the respective future and present-day periods respective to each model are shown. The scale is not the uniform to better appreciate the climate signal from each model

where the islands are located, and particularly in MAM. The changes in 2-meter mean temperature, as projected by the two intermediate simulations (CMCC at 22 km and ETH at 12 km grid spacings) in Fig. 9 (subplot c), lead to a coherent temperature signal with their respective GCM forcing data in all seasons. CMCC is warmer by 1−1.5 K in most of the domain than ETH. It is slightly colder-to-neutral along the Moroccan coast, which is in agreement with the GCMs. These intermediate-simulation results affect the km-scale results in Sect. 3.3.3. By comparing EC-EARTH with CMCC and MPI-ESM-LR with ETH, we notice that both the ETH and CMCC temperature projections follow those of the respective GCM (strong warming over land and northwest part of the domain). This is not surprising, as much of the computational domain considered is ocean, where the warming of the SST is prescribed to follow the GCM. This results in a warmer CMCC projection than ETH at km-scale resolution, which could be used as a justification, as the respective forcing data differ with respect to period and climate sensitivity.

### 3.3.2 Precipitation

The future climate simulations of precipitation for the islands of Madeira, Tenerife and Fuerteventura are presented in the following and in the supplementary material. Figures 10a, b, 11a and b show the precipitation indices for the island of Madeira and Tenerife for the winter and fall seasons, respectively. Both km-scale simulations represent a decrease in hourly frequency in both seasons. In DJF, both models project a decrease in hourly precipitation intensity in the northeastern part of Madeira. For Tenerife, the intensity signal is scattered. Moreover, the CMCC model projects a strong decrease in mean and extreme precipitation compared to the ETH model. Over Madeira in SON, the CMCC model projects an increase in hourly intensity, mean and heavy precipitation with an intensified signal over the mountain peaks. In contrast, the ETH model projects a slight decrease in hourly intensity, a strong decrease in mean precipitation, particularly over mountains, and contrasting changes in heavy precipitation with an increase on the northern coast and a decrease over the mountains and in the southern part

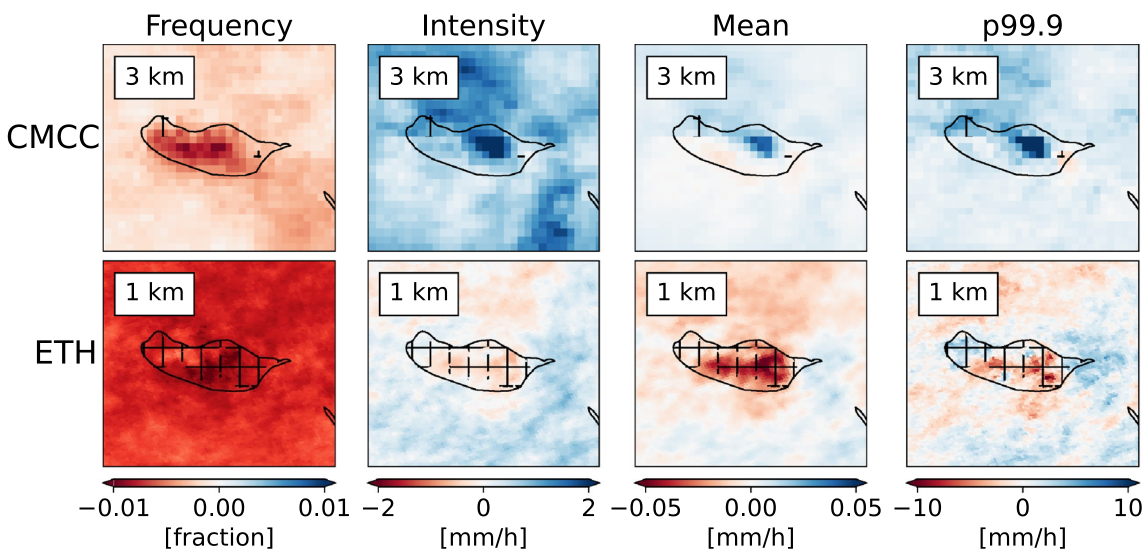


(a) Madeira

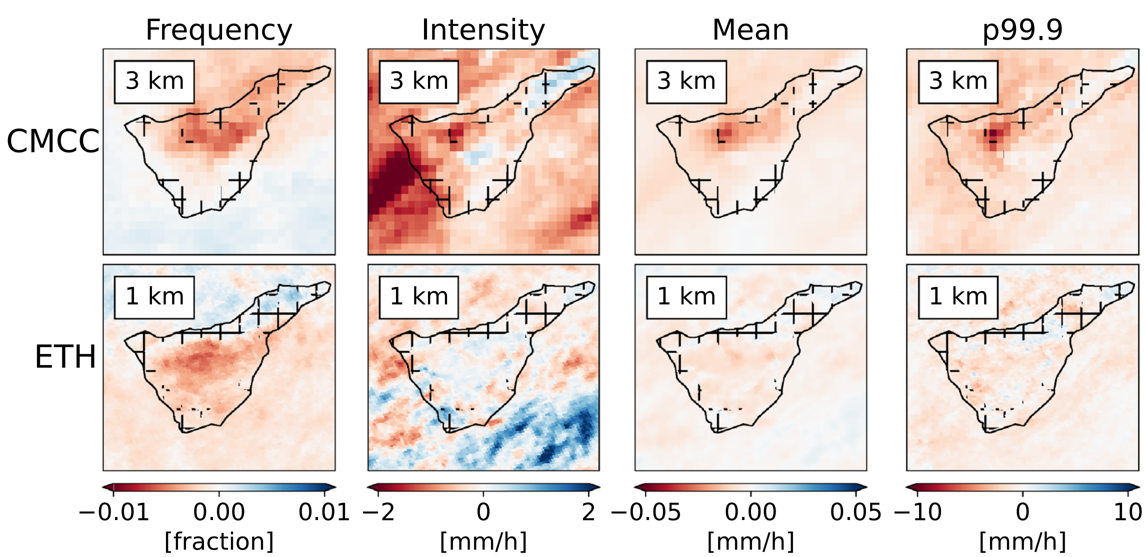


(b) Tenerife

**Fig. 11** As Fig. 10, but for the fall season (SON) of the island. Over Tenerife, both models agree in projecting a decrease of precipitation signals, more pronounced for CMCC model, except for an increase in intensity in the north-eastern corner of Tenerife. In other seasons, reported in the supplementary material, CMCC systematically projects a decrease in precipitation frequency, mean and heavy precipitation over the entire island of Madeira (Fig. A.20). Precipitation intensity tends to decrease on the northern coast and increase on the southern coast in both DJF and JJA. The ETH model does not project such large changes (Fig. A.21). The signal is generally weaker, and there is no systematic decrease or increase in the precipitation indices.

As for Madeira, over Tenerife (Figs. A.22 and A.23), both models agree in a general decrease in precipitation indices, particularly over orography, except for the JJA season, where ETH projects a neutral-to-cold signal. Over Fuerteventura (Figs. A.24 and A.25), both models agree on a decrease in frequency, mean and heavy precipitation in all seasons but SON, when CMCC projects an increase and ETH a decrease. Precipitation intensity is projected to increase in DJF and MAM and decrease in JJA and SON by CMCC. The ETH signals overall are very weak.

Figure 12 summarises the above results and allows a direct comparison between CMCC (red boxes) and ETH (blue boxes). On average, the two km-scale models tend to project a decrease (or no change) in all precipitation indices and in all seasons, which reinforces the finding that a decreased signal in precipitation dominates the Macaronesian islands. The reason behind the projected precipitation reduction could be due to different factors attributed to large-scale driving dynamical processes, such as a stronger subsidence associated to a northward extension of the Hadley cell circulation, or more local processes, such as the influence of the complex coastal upwelling systems (Carrillo et al. 2016; Vazquez et al. 2022; Gao et al. 2023). These aspects are not investigated in this study but highlight the relevance of detailed analyses and more comprehensive atmosphere-ocean regional coupled models to study the complex climate features of small islands located in the middle of the ocean. The models in Fig. 12 systematically agree on the changes in precipitation frequency and mean precipitation over all islands and seasons, although CMCC projects more pronounced changes than ETH, particularly in DJF. The spatial variability (represented by the distance between the

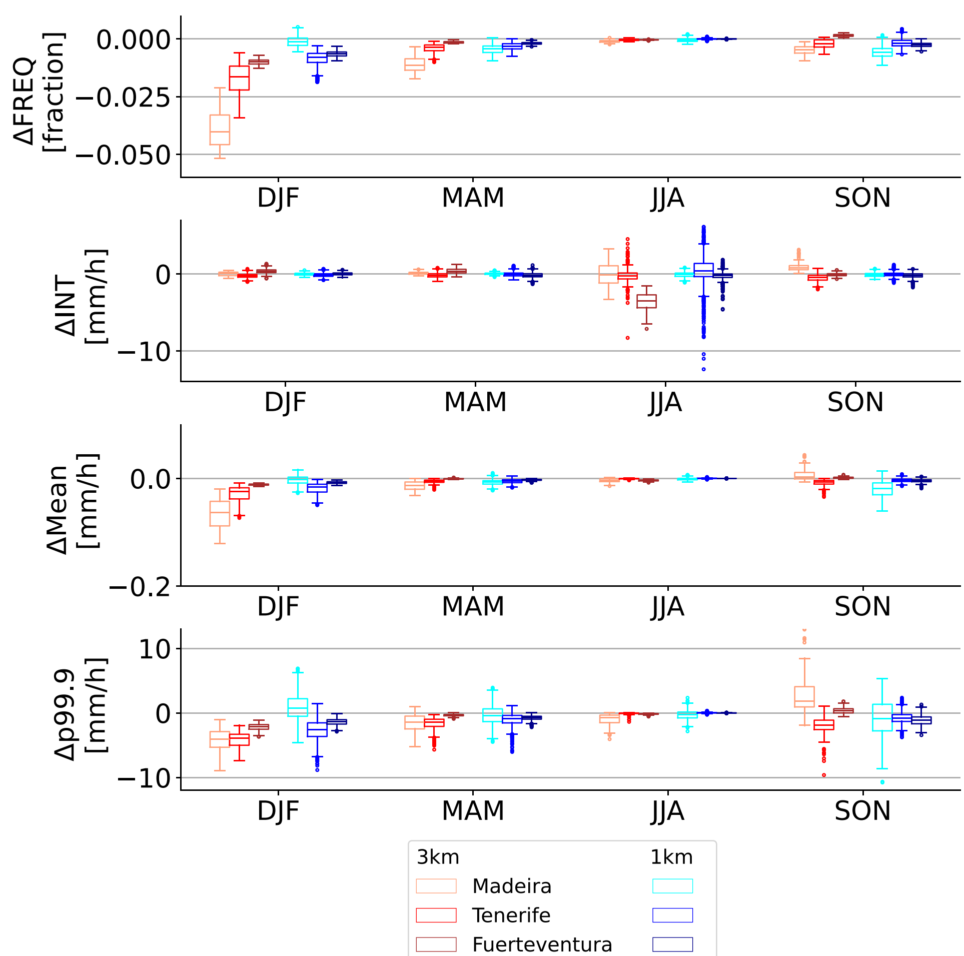


**Fig. 12** Box plots of the future changes in precipitation indices over each islands in all seasons. (From top to bottom): precipitation frequency, precipitation intensity, mean precipitation, and heavy precipitation as projected by the two km-scale models. The box plots with red and blue shadings show results for CMCC (3 km) and ETH (1 km) models, respectively. The differences were calculated over the respective future vs present-day periods of each model. Only grid points at a significance level of 5 % ($p < 0.05$) were considered

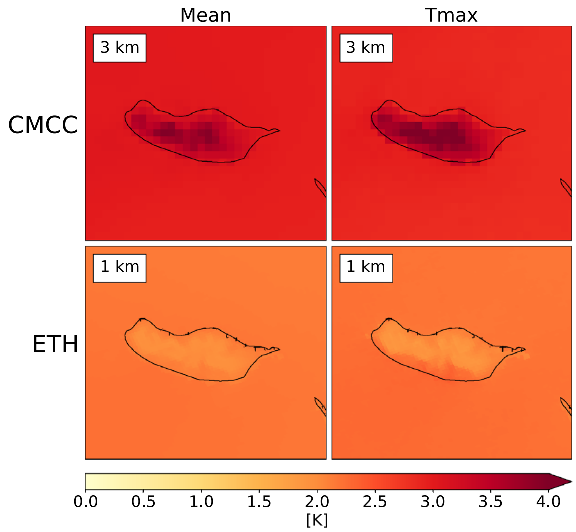


(a) Madeira, DJF

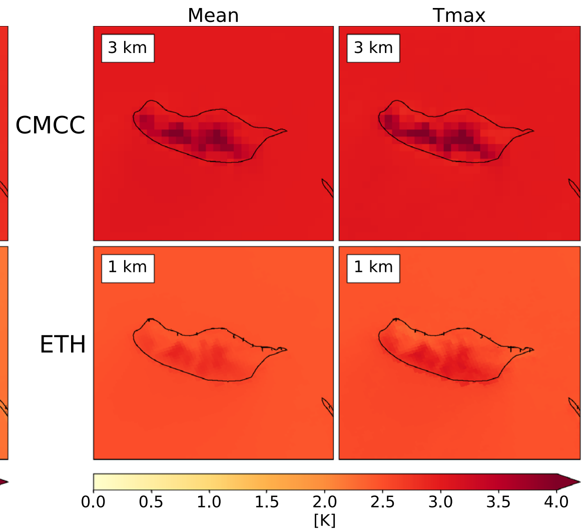


(b) Madeira, SON

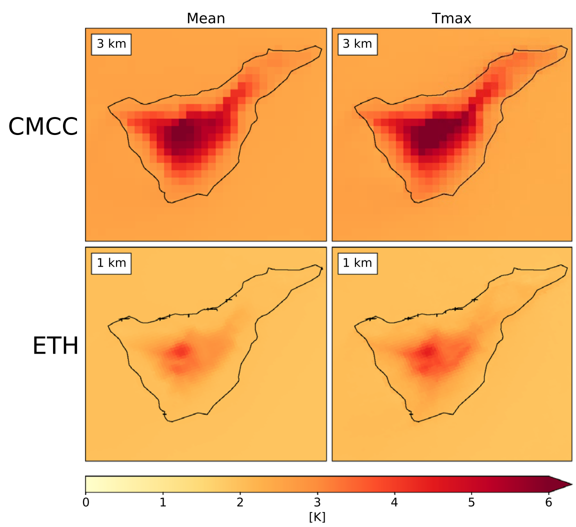


(c) Tenerife, DJF

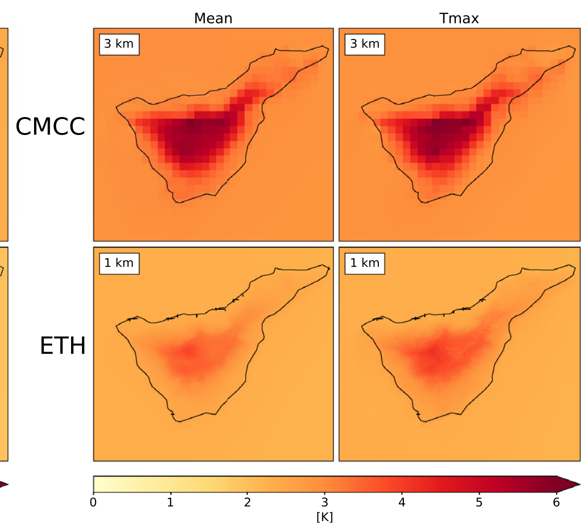


(d) Tenerife, SON

**Fig. 13** Changes in 2-meter temperature (mean) and mean of all daily maximum temperatures (Tmax) for (**a**), (**c**) winter (DJF) and (**b**), (**d**) fall (SON) as projected by the CMCC (3 km) and the ETH (1 km) models over the islands of (**a**), (**b**) Madeira and (**c**), (**d**) Tenerife. The differences between the future and the present periods respective to each model are shown. The color shadings show the temperature difference in Kelvin. The differences were calculated over the respective future vs present-day periods of each model. Note the different scales for the two islands

lower and upper whiskers of the boxes) tends to be larger over Madeira and Tenerife than over Fuerteventura in both CMCC and ETH, which is attributed to the spatial distribution of the signals over topography. The projected changes in hourly intensity are small in both models except in JJA when the signal is much more contrasted with a large spatial spread over the three islands, which is consistent with the simulations over the present-day climate (Fig. 5). The models also agree less in the projections of heavy precipitation (99.9th percentile), particularly in DJF and SON over Madeira. The spatial variability also tends to be larger in most seasons, particularly over Madeira and Tenerife. Overall, despite model disagreements that are analysed below, these results highlight a complex behaviour of precipitation over the three islands and emphasize the difficulties to project precipitation changes over such small islands without more comprehensive atmosphere-ocean regional coupled models.

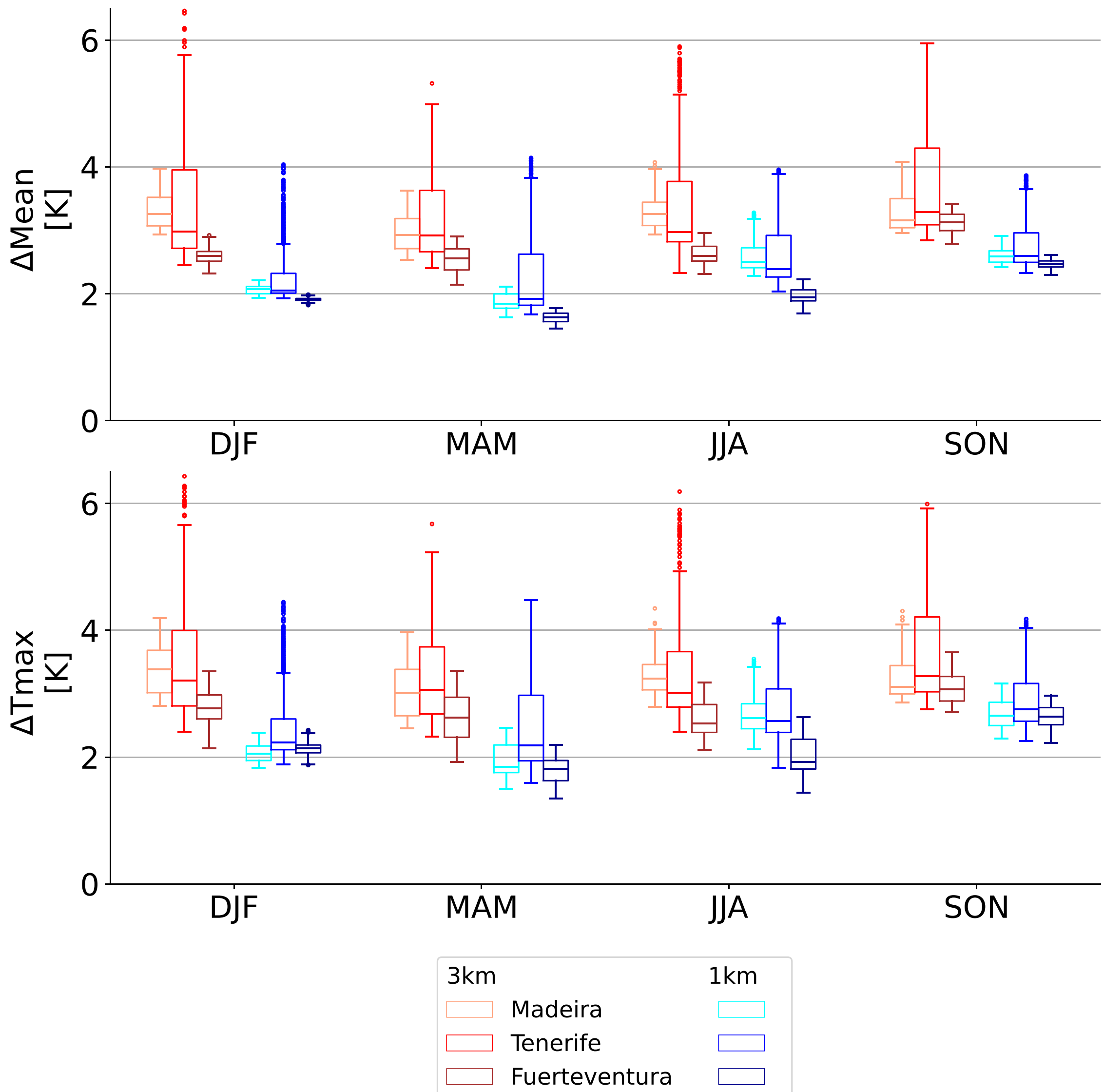


**Fig. 14** Box plots of future changes in temperature indices over each island in all seasons. (From top to bottom): 2-meter mean temperature and Tmax as projected by the two kilometer-scale models. The box plots with red and blue shadings show results for CMCC (3 km) and ETH (1 km) models, respectively. The indices were calculated over the respective future vs present-day periods of each model. Only grid points at a significance level of 5 % ($p < 0.05$) were considered

#### 3.3.3 Temperature

The projections of temperature for the islands of Madeira, Tenerife and Fuerteventura are presented in the following figures and in the supplementary material. Figure 13a–d show the future changes in the spatial distribution of 2-meter mean temperature and mean of daily maximum temperatures in Madeira and Tenerife for the winter and fall seasons, respectively. Both km-scale simulations project an increase in mean and maximum temperatures over the whole islands and in both seasons. The results reveal an elevation-dependent behaviour with a stronger temperature increase inside the island compared to the coastal areas. The CMCC model is generally much warmer than the ETH model by about 1–1.5 K. This finding is consistent across all seasons (Fig. A.26) and over all islands (Figs. A.27 and A2.8). The spatial relation of temperature increase with orography is also consistent and particularly pronounced in MAM and DJF over Madeira and Tenerife for the CMCC model. The elevation-dependent temperature behaviour over Tenerife and Madeira could be justified by the large-scale climate conditions (see Sect. 3.1), and is in agreement with previous studies (Bony et al. 2006; Hartmann et al. 2013; Expósito et al. 2015; Pérez et al. 2022). Such studies investigated that GCM projections indicate a greater warming at altitudes over Canary islands and highlighted an evidence, in summer, with the decrease in soil moisture that occurs over Tenerife, one of the most relevant local effects on temperature (Sangelantoni et al. 2024).

Figure 14 summarises the projections of 2-meter temperature indices for both km-scale models. As shown on the spatial maps, both models project an increase in temperature indices over all islands in all seasons. The increase is particularly strong in the CMCC model (with a median value around 3K in both mean and maximum temperatures) compared to the ETH model (median value around 2 K). The spatial variability is also very large for the two indices over Madeira and Tenerife in all seasons, particularly in CMCC (up to 3 K difference between the highest value and the median). Tenerife has the highest spatial variability in both models due to its high variability in topography (as shown in Fig. A.27), while the changes in temperature indices over Fuerteventura are smoother throughout the island. The models tend to show a slightly larger spatial variability in Tmax than in mean temperature over all islands and in all seasons.

### 3.3.4 Consistency between models results

Assessing the consistency in climate change sensitivity across km-scale simulations is key for exploring the added value of such models for local projections. The above results show a clear agreement between the CMCC and the ETH models in terms of temperature warming, although the scale of the increase is larger in the CMCC model than in the ETH model, which is further explored in Sect. 3.3.1. The consistency in precipitation indices is more difficult to assess due to their high spatial variability. In this section, we assess the consistency between CMCC and ETH simulations in terms of heavy precipitation changes with regards to future changes in mean temperature. Although inspired by the assessments of Held and Soden (2006) over the globe and Aalbers et al. (2018) over Europe, in this study, we look at seasonal means at the grid-point scale of precipitation changes and temperature increases over the three small-size islands from the two models, being aware that the highly dynamical system with orographic lifting and moisture transport from the sea affecting the Macaronesian islands are neglected. Figure 15 shows the projected changes in heavy precipitation versus 2-meter mean temperature in all seasons over each island. Specifically, the figure displays the changes in hourly heavy precipitation (p99.9) and 2-meter mean temperature projected by the two models over their respective periods (i.e. 2090–2099 vs 1996–2005 for CMCC, and 2106–2115 vs 2006–2015 for ETH). The seasonal mean was calculated by only considering inland grid cells (see Sect. 2).

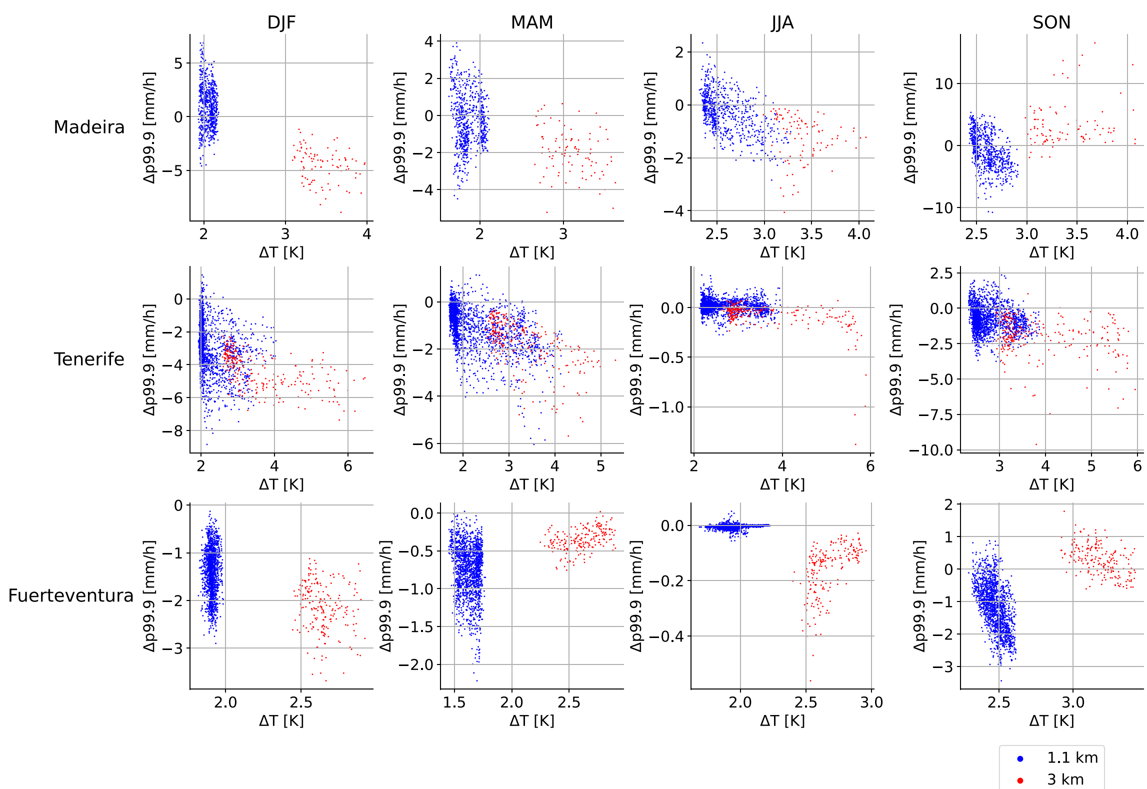


**Fig. 15** Change in heavy precipitation (99.9 percentile) vs. change in 2-meter mean temperature over each island and for each season. Each dot represents the difference between the respective future and present-day climates in both seasonal mean temperature and heavy precipitation over a land grid cell (with a land fraction above 50%)

Thus, the CMCC model (3 km) has a smaller number of grid points due to its coarser resolution compared to the ETH model (1 km). The warming signal projected by both models is almost uniform (except for Tenerife where the signal is narrow, probably due to its dependence on topographic height) while the signal in extreme precipitation varies much stronger. Overall, the two models tend to show a decrease in heavy precipitation with the warming of the islands. This is particularly clear in JJA over Madeira, in DJF, MAM and SON over Tenerife and in SON over Fuerteventura. These results are consistent with the changes in mean precipitation with increasing temperature (Figure A.29 in the supplementary material). The CMCC model usually shows a larger negative relationship between heavy precipitation and mean temperature than ETH (e.g. over Madeira in DJF and MAM, over Tenerife in JJA, over Fuerteventura in DJF). Although more data are needed to support a proper explanation, this could be partially due to its greater warming, associated to the SST effect, as shown in Fig. 9. The response of the heavy precipitation index over Madeira displays a greater spatial variability than the 2-meter temperature, especially for the ETH model in all seasons. There are a few clear disagreements between the two simulations. Over Madeira in SON, heavy precipitation decreases with increasing temperature in ETH but increases in CMCC. This is consistent with changes in mean precipitation (Fig. A.29 in the supplementary material). Over Fuerteventura in JJA, precipitation does not change with increasing temperature in ETH but increases in CMCC. This relationship is more pronounced in mean precipitation (Fig. A.29). This lack of relationship in ETH is attributed to high noise and the narrow projected changes in mean and heavy precipitation (Fig. A.25).

## 4 Conclusion

Enhancing the comprehension of present and future climate simulations at km-scale resolution is imperative within small island systems characterized by complex orography, as the Macaronesian islands. This is crucial to develop adaptation strategies and mitigation measures aimed at addressing the impact of climate change. Despite the high computational cost, the evident dependence of climate features on elevation underscores the necessity of employing high spatial resolution to accurately simulate complex rainfall and temperature patterns. This study assesses km-scale simulations over the Macaronesian islands (with a main focus on Madeira, Tenerife and Fuerteventura) using km-scale simulations from two regional climate models run by CMCC and ETH based on different modelling approaches. CMCC uses COSMO-CLM driven by EC-EARTH GCM (three-step nesting at 50, 25 and 3 km grid spacings) with a 10-year time-slice approach under the historical and RCP8.5 scenarios, and ETH uses COSMO-crCLIM driven by the ERA-Interim reanalysis (two-step nesting at 12 and 1 km grid spacings) with a pseudo-global warming approach driven by the MPI-ESM GCM under the RCP8.5 scenario to simulate the future climate. As the results are based on only two models with no common simulation strategy, it is not possible to provide reliable multi-model ensemble-like climate projections over the Macaronesian islands, as done over the Alpine region (Ban et al. 2021; Pichelli et al. 2021). Nonetheless, this exploratory study provides a first model inter-comparison at km-scale resolution over the Macaronesian domain. It faces the challenges that the regional climate modeling community has to cope with: how to reduce model uncertainties by exploiting the multiple and different downscaling techniques that are currently being developed (i.e. coupled dynamical models, emulators, machine learning, next generations GCMs with increased resolution).

The main outcomes of the study are reported in the following:

- It promotes the availability of high-resolution climate information over the Macaronesian region. Km-scale and hourly frequency climate information was missing and thus is particularly relevant to local climate services, policy makers and stakeholders. Due to their high computing costs, the length of the simulations are limited to 10 years. In 10-year time segments, natural climate variability cannot be properly represented, hampering the robustness of the climate projections. Furthermore, 10 years are not sufficient to adequately sample decadal to multi-decadal modes of variability such as the North Atlantic Oscillation that has a large influence on the Macaronesian climate variability (Mezzina et al. 2020). The presented simulations are therefore subject to uncertainties arising from natural climate variability (Lucas-Picher et al. 2021). As teleconnections may change in the future, longer simulations would be necessary. Nonetheless, users can benefit from this new set of simulations that show emerging signals that are not visible in lower resolution simulations.
- It provides insights into some scientific questions that are still unexplored due to lack of high-resolution gridded observations and high-resolution climate simulations over that territories. The current-day simulations are evaluated against available observations and reanalyses, with a focus on temperature and precipitation mean and extremes at km-scale resolution. The analyses reveal a spatial relation of precipitation indices with orography (with higher values over orography and weaker ones along the coast) over Madeira and Tenerife and a more uniform behaviour over the flat territory of Fuerteventura. So, a direct relationship is evident between the islands' heights and precipitation distribution (more mountain-

ous islands receive more precipitation, particularly on their windward sides), in agreement with previous studies based on station based measurements (Cropper and Hanna 2014). Compared to reanalysis and available observations, precipitation intensity and extremes are higher in all seasons, except in JJA. The two models, despite their different resolutions and simulation setups, show similar values for indices over each island and for each season, except in SON over Madeira. The diurnal cycle plots demonstrate that, in spite of some underestimations, km-scale models are able to simulate the shape of mean precipitation cycle over each island compared to observations, and so, this finding corroborates the ability of km-scale models demonstrated by previous studies over different areas (Ban et al. 2021; Adinolfi et al. 2020). The ETH model tends to be warmer than CMCC in all seasons over all islands, which is consistent with the driving ERA-Interim reanalysis being warmer than EC-EARTH GCM. This temperature difference over the islands aligns with the large-scale climate conditions of the Macaronesian domain in terms of surface pressure, winds, temperature and precipitation. Indeed, CMCC driven by EC-EARTH GCM simulates weaker northerly winds, colder near-surface and sea surface temperature over the Atlantic and the African coast and more precipitation in the northern part of the domain than the ETH model driven by ERA-Interim reanalysis.

- The future climate projections over the Canary and Madeira islands were investigated. Despite their different simulation strategies, both km-scale models generally agree on changes in hourly precipitation indices for the islands of Madeira, Tenerife and Fuerteventura: they simulate a decrease in precipitation frequency and in heavy and mean precipitation associated with a localised increase in intensity in JJA and SON. The greatest discrepancies between models, clearly due to the orography and driving conditions, occur more over Madeira and Tenerife and less over Fuerteventura. The models simulate an increase in 2-meter mean temperature by about 2–4 K over the islands, although the increase is slightly lower in the ETH model than CMCC in all seasons and over all islands, consistent with differences in the driving GCMs. The largest changes are simulated over mountains. There is no clear relationship between the warming and the hourly precipitation changes, possibly due to the complex topography of the islands. Some disagreements in the changes in precipitation emerge between the two simulations. Over Madeira in SON, heavy precipitation decreases with increasing temperature in ETH but increases in CMCC. Over Fuerteventura in JJA, precipitation does not change with increasing temperature in ETH but increases in CMCC. These inconsistencies are attributed to both the difference in the model resolution (precipitation tends to be noisier in ETH due to its higher resolution than CMCC) and the large-scale driving conditions. The changes in temperature simulated by the models at both intermediate and km-scale resolutions follow the changes projected by the GCMs with a stronger warming projected by EC-EARTH (that drives the CMCC model) than by MPI-ESM (that drives the ETH model). In spite of the different strategies and approaches, the changes in temperature and precipitation are consistent at km-scale between CMCC and ETH models over the islands in all seasons, with exception in autumn over Madeira. The use of km-scale simulations is demonstrated to be essential to properly represent temperature and precipitation signals over the Macaronesian islands, that are characterized by an elevation-dependent behaviour that is not consistently represented at coarser resolutions.

The km-scale climate simulations for both present-day and future climate conditions form the bedrock for more accurate and comprehensive climate change projections for the islands needed for impact studies, decision makings and the development of future adaptation strategies of the Macaronesian region. Climate data (such as remote sensing and ground-based observations, global and regional climate projections, seasonal or decadal predictions, statistical downscaling and hybrid approacheses) continue to increase over continental Europe, but small islands are commonly neglected. On the other hand, there is limited high-quality climate information due to the lack of coordinated modelling initiatives at km-scale over small islands and the need of coordinated, international collaborative effort to ensure that small island states and territories can move beyond sea-level rise impacts and understand their full spectrum of climate change-related risks is required (Evans et al. 2024). Moreover, over small island territories, coarse climate data and limited gridded observations represent a barrier for decision-making. The here presented simulations aim to underpin the current differences in country-to-country adaptation capability and ensure that European decision makers have access to detailed and accurate information, regardless of geographical location. These simulations fill a significant gap for local climate services, and the encouraging results highlight the need for further coordinated km-scale modelling initiatives. A suitable strategy to provide a robust ensemble and reduce uncertainties in climate projections over Macaronesian islands, would favour the usage of convection-permitting models with a spatial resolution in the range of 1–4 km (Lucas-Picher et al. 2021) and the definition of a protocol with common forcing data, nesting, domain, simulation set-up and periods. Therefore, a general suggestion coming from this study is that more effort is needed to coordinated initiatives in order to design effective adaptation and mitigation strategies of climate change effects on Macaronesian islands.

**Supplementary Information** The online version contains supplementary material available at https://doi.org/10.1007/s00382-024-07563-x.

**Acknowledgements** The authors acknowledge funding from the HORIZON 2020 EUCP (European Climate Prediction System) project (https://www.eucp-project.eu, grant agreement No. 776613). They gratefully acknowledge the WCRP-CORDEX-FPS on Convective phenomena at high resolution over Europe and the Mediterranean (FPS-CONV) and the research data exchange infrastructure and services provided by the Jülich Supercomputing Centre, Germany, as part of the Helmholtz Data Federation initiative. The ETH team (L.L., C.S., C.Z., M-E.D.) acknowledges the Partnership for Advanced Computing in Europe (PRACE) for awarding them access to Piz Daint at the Swiss National Supercomputing Centre (CSCS, Switzerland). They also acknowledge the Federal Office for Meteorology and Climatology (MeteoSwiss), the Swiss National Supercomputing Centre CSCS, the Center for Climate Systems Modeling (C2SM), and ETH Zürich for their contributions to the development and maintenance of the GPU-accelerated version of COSMO. The CMCC simulations have been performed using the COSMO model in CLimate Mode (COSMO-CLM) using CMCC Supercomputing Centre facilities. COSMO-CLM is the community model of the German regional climate research team, jointly further developed by the CLM-Community. M.A. acknowledges the members of the community for their common efforts to develop the model as well as P. Mercogliano, M. Raffa and E. Bucchignani. Acknowledgement is also for the World Climate Research Programme's Working Group on Regional Climate, and the Working Group on Coupled Modeling, former coordinating body of CORDEX and responsible panel for CMIP5. The authors are grateful to the Copernicus Climate Change Service (C3S), as ERA-Interim, ERA5 and UERRA data have been generated using Copernicus Climate Change Service Information and downloaded from the C3S Climate Data Store (CDS) platform. They acknowledge the data station agencies, Agencia Estatal de Meteorología (AEMET), the Instituto Português do Mar e da Atmosfera (IPMA) and the Delegação Regional da Madeira do IPMA for providing observed data of precipitation at hourly scale. A great thank is to Prof. Albano José González Fernández from Universidad de La Laguna en Tenerife and Prof. Pedro Soares from University of Lisbon for making us in contact with the national agencies.

**Author contributions** Conceptualisation, M. A. and M-E.D. ; methodology, M.A., M-E.D., C.Z, L.L. and C.S.; software, L.L., C.Z. and M.A.; validation, C.Z., L.L.; formal analysis, L.L.; investigation, M.A., M-E.D., L.L.and C.Z.; data curation, M.A., L.L. and C.Z.; writing original draft preparation, M.A.; writing, review and editing, M.A., M-E.D., L.L., C.Z., and C.S.; visualisation, L.L., C.Z. All authors have read and agreed to the published version of the manuscript.

**Funding** The climate simulations analysed in this work are funded by the HORIZON 2020 EUCP (European Climate Prediction System) project (https://www.eucp-project.eu, Grant Agreement No. 776613).

**Data availability** The simulations data will be available publicly on the Earth System Grid Federation (ESGF) under the CORDEX-FPSCONV project. Until then, data are available upon request.

## Declarations

**Conflict of interest** The authors declare that they have no conflict of interest.

**Ethical approval and consent to participate** Not applicable.

**Consent for publication** Not applicable.



## References

Aalbers EE, Lenderink G, Van Meijgaard E, Van Den Hurk BJJM (2018) Local-scale changes in mean and heavy precipitation in western Europe, climate change or internal variability? Clim Dyn 50(11):4745–4766. https://doi.org/10.1007/s00382-017-3901-9

Adinolfi M, Raffa M, Reder A, Mercogliano P (2020) Evaluation and expected changes of summer precipitation at convection permitting scale with COSMO-CLM over alpine space. Atmosphere 12(1):54. https://doi.org/10.3390/atmos12010054

Adinolfi M, Rianna G, Mercogliano P, Maiorano RMS, Aversa S (2021) Behaviour of energy piles under climate-change scenarios: a case study in southern Italy. Environ Geotech 8(8):571–585. https://doi.org/10.1680/jenge.19.00093

Adinolfi M, Raffa M, Reder A, Mercogliano P (2023) Investigation on potential and limitations of ERA5 reanalysis downscaled on Italy by a convection-permitting model. Clim Dyn. https://doi.org/10.1007/s00382-023-06803-w. (**Accessed 2023-06-15**)

Arakawa A, Lamb VR (1977) Computational design of the basic dynamical processes of the UCLA general circulation model. General Circ Models Atmos 17:173–265 (**Publisher: Methods in computational Physics**)

Baldauf M, Seifert A, Förstner J, Majewski D, Raschendorfer M, Reinhardt T (2011) Operational convective-scale numerical weather prediction with the COSMO model: description and sensitivities. Mon Weather Rev 139(12):3887–3905. https://doi.org/10.1175/MWR-D-10-05013.1

Ban N, Schmidli J, Schär C (2014) Evaluation of the convection-resolving regional climate modeling approach in decade-long simulations. J Geophys Res 119(13):7889–7907. https://doi.org/10.1002/2014JD021478

Ban N, Caillaud C, Coppola E, Pichelli E, Sobolowski S, Adinolfi M, Ahrens B, Alias A, Anders I, Bastin S, Belušić D, Berthou S, Brisson E, Cardoso RM, Chan SC, Christensen OB, Fernández J, Fita L, Frisius T, Gašparac G, Giorgi F, Goergen K, Haugen JE, Hodnebrog Ø, Kartsios S, Katragkou E, Kendon EJ, Keuler K, Lavin-Gullon A, Lenderink G, Leutwyler D, Lorenz T, Maraun D, Mercogliano P, Milovac J, Panitz H-J, Raffa M, Remedio AR, Schär C, Soares PMM, Srnec L, Steensen BM, Stocchi P, Tölle MH, Truhetz H, Vergara-Temprado J, De Vries H, Warrach-Sagi K, Wulfmeyer V, Zander MJ (2021) The first multi-model ensemble of regional climate simulations at kilometer-scale resolution, part I: evaluation of precipitation. Clim Dyn 57(1):275–302. https://doi.org/10.1007/s00382-021-05708-w

Beaugrand G (2009) Decadal changes in climate and ecosystems in the north Atlantic ocean and adjacent seas. Deep Sea Res Part II 56(8):656–673. https://doi.org/10.1016/j.dsr2.2008.12.022

Benevolenza MA, DeRigne L (2019) The impact of climate change and natural disasters on vulnerable populations: a systematic review of literature. J Hum Behav Soc Environ 29(2):266–281. https://doi.org/10.1080/10911359.2018.1527739

Benjamini Y, Hochberg Y (1995) Controlling the false discovery rate: a practical and powerful approach to multiple testing. J R Stat Soc Ser B Stat Methodol 57(1):289–300. https://doi.org/10.1111/j.2517-6161.1995.tb02031.x

Bony S, Colman R, Kattsov VM, Allan RP, Bretherton CS, Dufresne J-L, Hall A, Hallegatte S, Holland MM, Ingram W, Randall DA, Soden BJ, Tselioudis G, Webb MJ (2006) How well do we understand and evaluate climate change feedback processes? J Clim 19(15):3445–3482. https://doi.org/10.1175/JCLI3819.1

Bott A (1989) A positive definite advection scheme obtained by nonlinear renormalization of the advective fluxes. Monthly Weather Rev 117(5):1006–1016. https://doi.org/10.1175/1520-0493(1989)117<1006:APDASO>2.0.CO;2

Brogli R, Kröner N, Sørland SL, Lüthi D, Schär C (2019) The role of hadley circulation and lapse-rate changes for the future European summer climate. J Clim 32(2):385–404. https://doi.org/10.1175/JCLI-D-18-0431.1

Brogli R, Heim C, Mensch J, Sørland SL, Schär C (2023) The pseudo-global-warming (PGW) approach: methodology, software package PGW4era5 v1.1, validation, and sensitivity analyses. Geosci Model Dev 16(3):907–926. https://doi.org/10.5194/gmd-16-907-2023

Bucchignani E, Montesarchio M, Zollo AL, Mercogliano P (2016) High-resolution climate simulations with "COSMO-CLM" over Italy: performance evaluation and climate projections for the 21st century. Int J Climatol 36(2):735–756. https://doi.org/10.1002/joc.4379

Bucchignani E, Mercogliano P, Panitz H-J, Montesarchio M (2018) Climate change projections for the middle east-north Africa domain with COSMO-CLM at different spatial resolutions. Adv Clim Chang Res 9(1):66–80. https://doi.org/10.1016/j.accre.2018.01.004

Carrillo J, Guerra JC, Cuevas E, Barrancos J (2016) Characterization of the marine boundary layer and the trade-wind inversion over the sub-tropical north Atlantic. Bound-Layer Meteorol 158(2):311–330. https://doi.org/10.1007/s10546-015-0081-1

Carrillo J, Pérez JC, Expósito FJ, Díaz JP, González A (2022) Projections of wildfire weather danger in the canary islands. Sci Rep 12(1):8093. https://doi.org/10.1038/s41598-022-12132-5

Carrillo J, Hernández-Barrera S, Expósito FJ, Díaz JP, González A, Pérez JC (2023) The uneven impact of climate change on drought with elevation in the canary islands. NPJ Clim Atmos Sci 6(1):31. https://doi.org/10.1038/s41612-023-00358-7

Copernicus (2023) Record temperatures in Madeira, Portugal. https://www.copernicus.eu/en/media/image-day-gallery/record-temperatures-madeira-portugal. Accessed 2023-07-19

Copernicus Climate Change Service, C.D.S.: UERRA regional reanalysis for Europe on single levels from 1961 to 2019. Copernicus Climate Change Service (C3S) Climate Data Store (CDS). https://cds.climate.copernicus.eu/cdsapp#!/dataset/reanalysis-uerra-europe-single-levels?tab=overview. Accessed 2023-11-27

Coppola E, Sobolowski S, Pichelli E, Raffaele F, Ahrens B, Anders I, Ban N, Bastin S, Belda M, Belusic D, Caldas-Alvarez A, Cardoso RM, Davolio S, Dobler A, Fernandez J, Fita L, Fumiere Q, Giorgi F, Goergen K, Güttler I, Halenka T, Heinzeller D, Hodnebrog Ø, Jacob D, Kartsios S, Katragkou E, Kendon E, Khodayar S, Kunstmann H, Knist S, Lavín-Gullón A, Lind P, Lorenz T, Maraun D, Marelle L, Van Meijgaard E, Milovac J, Myhre G, Panitz H-J, Piazza M, Raffa M, Raub T, Rockel B, Schär C, Sieck K, Soares PMM, Somot S, Srnec L, Stocchi P, Tölle MH, Truhetz H, Vautard R, De Vries H, Warrach-Sagi K (2020) A first-of-its-kind multi-model convection permitting ensemble for investigating convective phenomena over Europe and the mediterranean. Clim Dyn 55(1):3–34. https://doi.org/10.1007/s00382-018-4521-8

Cropper TE, Hanna E (2014) An analysis of the climate of Macaronesia, 1865–2012. Int J Climatol 34(3):604–622. https://doi.org/10.1002/joc.3710

Doms G, Baldauf M (2021) A description of the non-hydrostatic regional COSMO-model, part I: dynamics and numerics. DWD, Offenbach. http://cosmo-model.org/content/model/documentation/core/default.htm#p1

ECMWF: ERA-Interim | ECMWF. https://www.ecmwf.int/en/forecasts/datasets/reanalysis-datasets/era-interim

Espinosa LA, Portela MM (2020) Rainfall trends over a small island teleconnected to the north Atlantic oscillation—the case of madeira island, Portugal. Water Resour Manage 34(14):4449–4467. https://doi.org/10.1007/s11269-020-02668-4

Evans JP, Belmadani A, Menkes C, Stephenson T, Thatcher M, Gibson PB, Peltier A (2024) Higher-resolution projections needed for small island climates. Nat Clim Chang 14(7):668–670. https://doi.org/10.1038/s41558-024-02028-9

Expósito FJ, González A, Pérez JC, Díaz JP, Taima D (2015) High-resolution future projections of temperature and precipitation in the canary islands. J Clim 28(19):7846–7856. https://doi.org/10.1175/JCLI-D-15-0030.1

Fosser G, Gaetani M, Kendon EJ, Adinolfi M, Ban N, Belušić D, Caillaud C, Careto JAM, Coppola E, Demory M-E, De Vries H, Dobler A, Feldmann H, Goergen K, Lenderink G, Pichelli E, Schär C, Soares PMM, Somot S, Tölle MH (2024) Convection-permitting climate models offer more certain extreme rainfall projections. NPJ Clim Atmos Sci 7(1):51. https://doi.org/10.1038/s41612-024-00600-w

Fragoso M, Trigo RM, Pinto JG, Lopes S, Lopes A, Ulbrich S, Magro C (2012) The 20 February 2010 madeira flash-floods: synoptic analysis and extreme rainfall assessment. Nat Hazard 12(3):715–730. https://doi.org/10.5194/nhess-12-715-2012

Fuhrer O, Osuna C, Lapillonne X, Gysi T, Bianco M, Arteaga A, Schulthess TC (2014) Towards a performance portable, architecture agnostic implementation strategy for weather and climate models. Supercomput Front Innov 1(1):44–61. https://doi.org/10.14529/jsfi140103

Fuhrer O, Chadha T, Hoefler T, Kwasniewski G, Lapillonne X, Leutwyler D, Lüthi D, Osuna C, Schär C, Schulthess TC, Vogt H (2018) Near-global climate simulation at 1 km resolution: establishing a performance baseline on 4888 GPUs with COSMO 5.0 km. Geosci Model Dev 11(4):1665–1681. https://doi.org/10.5194/gmd-11-1665-2018

Gallin L (2021) Berenberg says European floods to cost reinsurers up to 3bn. https://www.reinsurancene.ws/berenberg-says-european-floods-to-cost-reinsurers-up-to-e3bn/

Gao Q, Zeman C, Vergara-Temprado J, Lima DCA, Molnar P, Schär C (2023) Vortex streets to the lee of madeira in a kilometre-resolution regional climate model. Weather Clim Dyn 4(1):189–211. https://doi.org/10.5194/WCD-4-189-2023

Giorgetta MA, Jungclaus J, Reick CH, Legutke S, Bader J, Böttinger M, Brovkin V, Crueger T, Esch M, Fieg K, Glushak K, Gayler V, Haak H, Hollweg H, Ilyina T, Kinne S, Kornblueh L, Matei D, Mauritsen T, Mikolajewicz U, Mueller W, Notz D, Pithan F, Raddatz T, Rast S, Redler R, Roeckner E, Schmidt H, Schnur R, Segschneider J, Six KD, Stockhause M, Timmreck C, Wegner J, Widmann H, Wieners K, Claussen M, Marotzke J, Stevens B (2013) Climate and carbon cycle changes from 1850 to 2100 in MPI-ESM simulations for the coupled model intercomparison

project phase 5. J Adv Model Earth Syst 5(3):572–597. https://doi.org/10.1002/jame.20038
Giorgi F, Mearns LO (1999) Introduction to special section: regional climate modeling revisited. J Geophys Res 104:6335–6352. https://doi.org/10.1029/98JD02072
Giorgi F, Jones C, Asrar GR (2009) Addressing climate information needs at the regional level: the CORDEX framework. WMO Bull 58(3):175–183
Giorgi F, Raffaele F, Coppola E (2019) The response of precipitation characteristics to global warming from climate projections. Earth Syst Dyn 10(1):73–89. https://doi.org/10.5194/esd-10-73-2019
Gustafsson N, Berre L, Hornquist S, Huang X-Y, Lindskog M, Navascues B, Mogensen KS, Thorsteinsson S (2001) Three-dimensional variational data assimilation for a limited area model. Part I: general formulation and the background error constraint. Tellus A 53(4):425–446. https://doi.org/10.1111/j.1600-0870.2001.00425.x
Hall A (2014) Projecting regional change. Science 346(6216):1461–1462. https://doi.org/10.1126/science.aaa0629
Hartmann DL, Klein Tank AMG, Rusticucci M, Alexander LV, Brönnimann S, Rahman Charabi YA, Dentener FJ, Dlugokencky EJ, Easterling DR, Kaplan A, Soden BJ, Thorne PW, Wild M, Zhai P (2013) Climate change 2013 the physical science basis 9781107057999, 159–254
Heise E, Ritter B, Schrodin R, Wetterdienst D (2006) Operational implementation of the multilayer soil model. Citeseer
Held IM, Soden BJ (2006) Robust responses of the hydrological cycle to global warming. J Clim 19(21):5686–5699. https://doi.org/10.1175/JCLI3990.1
Herrera RG, Puyol DG, Martín EH, Presa LG, Rodríguez PR (2001) Influence of the north atlantic oscillation on the canary islands precipitation. J Clim 14(19):3889–3903. https://doi.org/10.1175/1520-0442(2001)014%3C3889:IOTNAO%3E2.0.CO;2
Hersbach H, Bell B, Berrisford P, Hirahara S, Horányi A, Muñoz-Sabater J, Nicolas J, Peubey C, Radu R, Schepers D, Simmons A, Soci C, Abdalla S, Abellan X, Balsamo G, Bechtold P, Biavati G, Bidlot J, Bonavita M, De Chiara G, Dahlgren P, Dee D, Diamantakis M, Dragani R, Flemming J, Forbes R, Fuentes M, Geer A, Haimberger L, Healy S, Hogan RJ, Hólm E, Janisková M, Keeley S, Laloyaux P, Lopez P, Lupu C, Radnoti G, De Rosnay P, Rozum I, Vamborg F, Villaume S, Thépaut J (2020) The ERA5 global reanalysis. Q J R Meteorol Soc 146(730):1999–2049. https://doi.org/10.1002/qj.3803
Hewitt CD, Lowe JA (2018) Toward a European climate prediction system. Bull Am Meteor Soc 99(10):1997–2001. https://doi.org/10.1175/BAMS-D-18-0022.1
Jacob D, Teichmann C, Sobolowski S, Katragkou E, Anders I, Belda M, Benestad R, Boberg F, Buonomo E, Cardoso RM, Casanueva A, Christensen OB, Christensen JH, Coppola E, De Cruz L, Davin EL, Dobler A, Domínguez M, Fealy R, Fernandez J, Gaertner MA, García-Díez M, Giorgi F, Gobiet A, Goergen K, Gómez-Navarro JJ, Alemán JJG, Gutiérrez C, Gutiérrez JM, Güttler I, Haensler A, Halenka T, Jerez S, Jiménez-Guerrero P, Jones RG, Keuler K, Kjellström E, Knist S, Kotlarski S, Maraun D, Van Meijgaard E, Mercogliano P, Montávez JP, Navarra A, Nikulin G, De Noblet-Ducoudré N, Panitz H-J, Pfeifer S, Piazza M, Pichelli E, Pietikäinen J-P, Prein AF, Preuschmann S, Rechid D, Rockel B, Romera R, Sánchez E, Sieck K, Soares PMM, Somot S, Srnec L, Sørland SL, Termonia P, Truhetz H, Vautard R, Warrach-Sagi K, Wulfmeyer V (2020) Regional climate downscaling over Europe: perspectives from the EURO-CORDEX community. Reg Environ Change 20(2):51. https://doi.org/10.1007/s10113-020-01606-9
Jerez S, López-Romero JM, Turco M, Lorente-Plazas R, Gómez-Navarro JJ, Jiménez-Guerrero P, Montávez JP (2020) On the spin-up period in WRF simulations over Europe: trade-offs between length and seasonality. J Adv Model Earth Syst 12(4):2019–001945. https://doi.org/10.1029/2019MS001945
Karnauskas KB, Donnelly JP, Anchukaitis KJ (2016) Future freshwater stress for island populations. Nat Clim Chang 6(7):720–725. https://doi.org/10.1038/nclimate2987
Kawase H, Yoshikane T, Hara M, Ailikun B, Kimura F, Yasunari T (2008) Downscaling of the climatic change in the mei-yu rainband in east Asia by a pseudo climate simulation method. SOLA 4:73–76. https://doi.org/10.2151/sola.2008-019
Kerr RA (2011) Vital details of global warming are eluding forecasters. Science 334(6053):173–174. https://doi.org/10.1126/science.334.6053.173
Kerr RA (2013) Forecasting regional climate change flunks its first test. Science 339(6120):638–638. https://doi.org/10.1126/science.339.6120.638
Kinne S, Schulz M, Textor C, Guibert S, Balkanski Y, Bauer SE, Berntsen T, Berglen TF, Boucher O, Chin M, Collins W, Dentener F, Diehl T, Easter R, Feichter J, Fillmore D, Ghan S, Ginoux P, Gong S, Grini A, Hendricks J, Herzog M, Horowitz L, Isaksen I, Iversen T, Kirkevåg A, Kloster S, Koch D, Kristjansson JE, Krol M, Lauer A, Lamarque JF, Lesins G, Liu X, Lohmann U, Montanaro V, Myhre G, Penner J, Pitari G, Reddy S, Seland O, Stier P, Takemura T, Tie X (2006) An AeroCom initial assessment—optical properties in aerosol component modules of global models. Atmos Chem Phys 6(7):1815–1834. https://doi.org/10.5194/acp-6-1815-2006
Klemp JB, Dudhia J, Hassiotis AD (2008) An upper gravity-wave absorbing layer for NWP applications. Mon Weather Rev 136(10):3987–4004. https://doi.org/10.1175/2008MWR2596.1
Lavin-Gullon A, Milovac J, García-Díez M, Fernández J (2023) Spin-up time and internal variability analysis for overlapping time slices in a regional climate model. Clim Dyn 61(1):47–64. https://doi.org/10.1007/s00382-022-06560-2
Leutwyler D, Lüthi D, Ban N, Fuhrer O, Schär C (2017) Evaluation of the convection-resolving climate modeling approach on continental scales. J Geophys Res 122(10):5237–5258 (**Publisher: Wiley Online Library**)
Leutwyler D, Lüthi D, Ban N, Fuhrer O, Schär C (2017) Evaluation of the convection-resolving climate modeling approach on continental scales. J Geophys Res 122(10):5237–5258. https://doi.org/10.1002/2016JD026013
Lucas-Picher P, Argüeso D, Brisson E, Tramblay Y, Berg P, Lemonsu A, Kotlarski S, Caillaud C (2021) Convection-permitting modeling with regional climate models: latest developments and next steps. WIREs Clim Change 12(6):731. https://doi.org/10.1002/wcc.731
Mann HB, Whitney DR (1947) On a test of whether one of two random variables is stochastically larger than the other. Ann Math Stat 18(1):50–60
Mezzina B, García-Serrano J, Bladé I, Kucharski F (2020) Dynamics of the ENSO teleconnection and NAO variability in the north Atlantic–European late winter. J Clim 33(3):907–923. https://doi.org/10.1175/JCLI-D-19-0192.1
Mohr S, Ehret U, Kunz M, Ludwig P, Caldas-Alvarez A, Daniell JE, Ehmele F, Feldmann H, Franca MJ, Gattke C, Hundhausen M, Knippertz P, Küpfer K, Mühr B, Pinto JG, Quinting J, Schäfer AM, Scheibel M, Seidel F, Wisotzky C (2023) A multi-disciplinary analysis of the exceptional flood event of July 2021 in central Europe—part 1: event description and analysis. Nat Hazard 23(2):525–551. https://doi.org/10.5194/nhess-23-525-2023
Molina MO, Careto JM, Gutiérrez C, Sánchez E, Goergen K, Sobolowski S, Coppola E, Pichelli E, Ban N, Belušić D, Short C, Caillaud C, Dobler A, Hodnebrog Ø, Kartsios S, Lenderink G, De Vries H, Göktürk O, Milovac J, Feldmann H, Truhetz H, Demory ME, Warrach-Sagi K, Keuler K, Adinolfi M, Raffa M, Tölle M, Sieck K, Bastin S, Soares PMM (2024) The added value of simulated near-surface wind speed over the alps from

a km-scale multimodel ensemble. Clim Dyn. https://doi.org/10.1007/s00382-024-07257-4

Mountain Research Initiative EDW Working Group (2015) Elevation-dependent warming in mountain regions of the world. Nat Clim Change 5(5):424–430. https://doi.org/10.1038/nclimate2563. Accessed 2023-10-13

Peral García C, Navascués Fernández-Victorio B, Ramos Calzado P (2017) Serie de Precipitación Diaria en Rejilla Con Fines Climáticos. Agencia Estatal de Meteorología. https://doi.org/10.31978/014-17-009-5. http://www.aemet.es/es/conocermas/recursos_en_linea/publicaciones_y_estudios/publicaciones/detalles/NT_24_AEMET Accessed 2024-06-24

Pérez JC, Díaz JP, González A, Expósito J, Rivera-López F, Taima D (2014) Evaluation of WRF parameterizations for dynamical downscaling in the canary islands. J Clim 27(14):5611–5631. https://doi.org/10.1175/JCLI-D-13-00458.1

Pérez JC, Expósito FJ, González A, Díaz JP (2022) Climate projections at a convection-permitting scale of extreme temperature indices for an archipelago with a complex microclimate structure. Weather Clim Extremes 36:100459. https://doi.org/10.1016/j.wace.2022.100459

Pichelli E, Coppola E, Sobolowski S, Ban N, Giorgi F, Stocchi P, Alias A, Belušić D, Berthou S, Caillaud C, Cardoso RM, Chan S, Christensen OB, Dobler A, De Vries H, Goergen K, Kendon EJ, Keuler K, Lenderink G, Lorenz T, Mishra AN, Panitz H-J, Schär C, Soares PMM, Truhetz H, Vergara-Temprado J (2021) The first multi-model ensemble of regional climate simulations at kilometer-scale resolution part 2: historical and future simulations of precipitation. Clim Dyn 56(11):3581–3602. https://doi.org/10.1007/s00382-021-05657-4

Prein AF, Langhans W, Fosser G, Ferrone A, Ban N, Goergen K, Keller M, Tölle M, Gutjahr O, Feser F, Brisson E, Kollet S, Schmidli J, Van Lipzig NPM, Leung R (2015) A review on regional convection-permitting climate modeling: demonstrations, prospects, and challenges. Rev Geophys 53(2):323–361. https://doi.org/10.1002/2014RG000475

Raschendorfer M (2001) The new turbulence parametrization of LM. COSMO Newsletter No. 1:90-98. http://www.cosmo-model.org/content/model/documentation/newsLetters/default.htm

Reinhardt T, Seifert A (2006) A three-category ice scheme for LMK. Cosmo Newslett 6:115–120

Riahi K, Rao S, Krey V, Cho C, Chirkov V, Fischer G, Kindermann G, Nakicenovic N, Rafaj P (2011) RCP 8.5-a scenario of comparatively high greenhouse gas emissions. Clim Change 109(1):33–57. https://doi.org/10.1007/s10584-011-0149-y

Ritter B, Geleyn J-F (1992) A comprehensive radiation scheme for numerical weather prediction models with potential applications in climate simulations. Monthly Weather Rev 120(2):303–325. https://doi.org/10.1175/1520-0493(1992)120%3C0303:ACRSFN%3E2.0.CO;2

Rockel B, Will A, Hense A (2008) The regional climate model COSMO-CLM (CCLM). Meteorol Z 17(4):347–348. https://doi.org/10.1127/0941-2948/2008/0309

Rummukainen M (2009) State-of-the-art with regional climate models. WIREs Clim Change 1(1):82–96

Sangelantoni L, Sobolowski S, Lorenz T, Hodnebrog Ø, Cardoso RM, Soares PMM, Ferretti R, Lavín-Gullón A, Fernandez J, Goergen K, Milovac J, Katragkou E, Kartsios S, Coppola E, Pichelli E, Adinolfi M, Mercogliano P, Berthou S, De Vries H, Dobler A, Belušić D, Feldmann H, Tölle MH, Bastin S (2024) Investigating the representation of heatwaves from an ensemble of km-scale regional climate simulations within CORDEX-FPS convection. Clim Dyn 62(6):4635–4671. https://doi.org/10.1007/s00382-023-06769-9

Schär C, Frei C, Lüthi D, Davies HC (1996) Surrogate climate-change scenarios for regional climate models. Geophys Res Lett 23(6):669–672. https://doi.org/10.1029/96GL00265

Schär C, Fuhrer O, Arteaga A, Ban N, Charpilloz C, Di Girolamo S, Hentgen L, Hoefler T, Lapillonne X, Leutwyler D, Osterried K, Panosetti D, Rüdisühli S, Schlemmer L, Schulthess TC, Sprenger M, Ubbiali S, Wernli H (2020) Kilometer-scale climate models: prospects and challenges. Bull Am Meteor Soc 101(5):567–587. https://doi.org/10.1175/BAMS-D-18-0167.1

Schiermeier Q (2010) The real holes in climate science. Nature 463(7279):284–287. https://doi.org/10.1038/463284a

Schlemmer L, Schär C, Lüthi D, Strebel L (2018) A groundwater and runoff formulation for weather and climate models. J Adv Model Earth Syst 10(8):1809–1832. https://doi.org/10.1029/2017MS001260

Sørland SL, Schär C, Lüthi D, Kjellström E (2018) Bias patterns and climate change signals in GCM-RCM model chains. Environ Res Lett 13(7):074017. https://doi.org/10.1088/1748-9326/aacc77

Steppeler J, Doms G, Schättler U, Bitzer HW, Gassmann A, Damrath U, Gregoric G (2003) Meso-gamma scale forecasts using the non-hydrostatic model LM. Meteorol Atmos Phys 82(1):75–96. https://doi.org/10.1007/s00703-001-0592-9

Tiedtke M (1989) A comprehensive mass flux scheme for cumulus parameterization in large-scale models. Monthly Weather Rev 117(8):1779–1800. https://doi.org/10.1175/1520-0493(1989)117%3C1779:ACMFSF%3E2.0.CO;2

Uncertainties in Ensembles of Regional Re-Analyses (2017) Deliverable D2.7 HARMONIE Reanalysis Report of Results and Dataset. http://www.uerra.eu/component/dpattachments/?task=attachment.download&id=296

Varela R, Rodríguez-Díaz L, De Castro M, Gómez-Gesteira M (2022) Influence of canary upwelling system on coastal SST warming along the 21st century using CMIP6 GCMs. Global Planet Change 208:103692. https://doi.org/10.1016/j.gloplacha.2021.103692

Vazquez R, Parras-Berrocal I, Cabos W, Sein DV, Mañanes R, Izquierdo A (2022) Assessment of the canary current upwelling system in a regionally coupled climate model. Clim Dyn 58(1):69–85. https://doi.org/10.1007/s00382-021-05890-x

Weather and climate extreme events in a changing climate. In: Intergovernmental Panel on Climate Change (IPCC) (ed.) Climate Change 2021 - The Physical Science Basis: Working Group I Contribution to the Sixth Assessment Report of the Intergovernmental Panel on Climate Change, pp 1513–1766. Cambridge University Press. https://doi.org/10.1017/9781009157896.013. https://www.cambridge.org/core/books/climate-change-2021-the-physical-science-basis/weather-and-climate-extreme-events-in-a-changing-climate/5BCB24C5699F1D42B2DE379BDD4E2119. Accessed 2024-10-22

Wicker LJ, Skamarock WC (2002) Time-splitting methods for elastic models using forward time schemes. Monthly Weather Rev 130(8):2088–2097. https://doi.org/10.1175/1520-0493(2002)130%3C2088:TSMFEM%3E2.0.CO;2

Wilks DS (2016) “The stippling shows statistically significant grid points’’: How research results are routinely overstated and overinterpreted, and what to do about it. Bull Am Meteor Soc 97(12):2263–2273. https://doi.org/10.1175/BAMS-D-15-00267.1

Zeman C, Schär C (2022) An ensemble-based statistical methodology to detect differences in weather and climate model executables. Geosci Model Dev 15(8):3183–3203. https://doi.org/10.5194/gmd-15-3183-2022

Zittis G, Hadjinicolaou P, Almazroui M, Bucchignani E, Driouech F, El Rhaz K, Kurnaz L, Nikulin G, Ntoumos A, Ozturk T, Proestos Y, Stenchikov G, Zaaboul R, Lelieveld J (2021) Business-as-usual will lead to super and ultra-extreme heatwaves in the middle east and north Africa. NPJ Clim Atmos Sci 4(1):20. https://doi.org/10.1038/s41612-021-00178-7

**Publisher's Note** Springer Nature remains neutral with regard to jurisdictional claims in published maps and institutional affiliations.